The Plant Cell, Vol. 32: 3978–4001, December 2020, www.plantcell.org © 2020 ASPB.

The Cotton Wall-Associated Kinase GhWAK7A Mediates Responses to Fungal Wilt Pathogens by Complexing with the Chitin Sensory Receptors[OPEN]

Ping Wang,[a,b] Lin Zhou,[c] Pierce Jamieson,[a] Lin Zhang,[c] Zhixue Zhao,[a] Kevin Babilonia,[c] Wenyong Shao,[c,d] Lizhu Wu,[c,d] Roma Mustafa,[c,e] Imran Amin,[e] Alessandra Diomaiuti,[f] Daniela Pontiggia,[f] Simone Ferrari,[f] Yuxia Hou,[b] Ping He,[c] and Libo Shan[a,1]

[a] Department of Plant Pathology and Microbiology, and Institute for Plant Genomics and Biotechnology, Texas A&M University, College Station, Texas 77843

[b] College of Science, China Agricultural University, Beijing 100193, China

[c] Department of Biochemistry and Biophysics, and Institute for Plant Genomics and Biotechnology, Texas A&M University, College Station, Texas 77843

[d] North China Key Laboratory for Germplasm Resources of Education Ministry, Hebei Agricultural University, Baoding, Hebei 071001, China

[e] Agricultural Biotechnology Division, National Institute for Biotechnology and Genetic Engineering, Faisalabad, Punjab, 44000 Pakistan

[f] Università di Roma Sapienza, Dipartimento di Biologia e Biotecnologie "Charles Darwin," 00185 Roma, Italy

ORCID IDs: 0000-0002-4881-2804 (P.W.); 0000-0002-1010-5610 (L.Z.); 0000-0001-5929-5534 (P.J.); 0000-0002-5070-7667 (L.Z.); 0000-0002-3450-8422 (Z.X.Z.); 0000-0002-2980-4526 (K.B.); 0000-0002-1824-2302 (W.Y.S.); 0000-0002-9324-6143 (L.H.W.); 0000-0002-8979-9044 (R.M.); 0000-0003-3063-4103 (I.A.); 0000-0002-3758-3743 (A.D.); 0000-0002-0980-107X (D.P.); 0000-0002-1389-2090 (S.F.); 0000-0003-2975-9953 (Y.X.H.); 0000-0002-5926-8349 (P.H.); 0000-0002-4798-9907 (L.S.)

Plant receptor-like kinases (RLKs) are important players in response to pathogen infections. Verticillium and Fusarium wilts, caused by *Verticillium dahliae* (*Vd*) and *Fusarium oxysporum* f. sp *vasinfectum* (*Fov*), respectively, are among the most devastating diseases in cotton (*Gossypium* spp). To understand the cotton response to these soil-borne fungal pathogens, we performed a genome-wide in silico characterization and functional screen of diverse RLKs for their involvement in cotton wilt diseases. We identified *Gossypium hirsutum* GhWAK7A, a wall-associated kinase, that positively regulates cotton response to both *Vd* and *Fov* infections. Chitin, the major constituent of the fungal cell wall, is perceived by lysin-motif-containing RLKs (LYKs/CERK1), leading to the activation of plant defense against fungal pathogens. A conserved chitin sensing and signaling system is present in cotton, including chitin-induced GhLYK5-GhCERK1 dimerization and phosphorylation, and contributes to cotton defense against *Vd* and *Fov*. Importantly, GhWAK7A directly interacts with both GhLYK5 and GhCERK1 and promotes chitin-induced GhLYK5-GhCERK1 dimerization. GhWAK7A phosphorylates GhLYK5, which itself does not have kinase activity, but requires phosphorylation for its function. Consequently, GhWAK7A plays a crucial role in chitin-induced responses. Thus, our data reveal GhWAK7A as an important component in cotton response to fungal wilt pathogens by complexing with the chitin receptors.

INTRODUCTION

In addition to its use in textile manufacturing, cotton (*Gossypium* spp) serves as an agro-economically important source of feed, foodstuff, oil, and biofuel. Within the genus *Gossypium*, there are 41 to 47 diploid species grouped into eight diploid genome groups (A through G, and K) and seven allotetraploid species, which were formed likely from interspecific hybridizations between the A-genome species resembling *G. herbaceum* or *G. arboreum* and the D-genome species *G. raimondii* (Zhang et al., 2008; Wang et al., 2018; Hu et al., 2019). After the polyploidization event, the allopolyploids gave rise to three modern lineages, including the agronomically important *G. hirsutum* and *G. barbadense* (Zhang et al., 2008; Wang et al., 2018). *G. hirsutum*, known as upland cotton, is the most widely cultivated species of cotton and constitutes ~90% of cotton output worldwide. The genome sequences of *G. raimondii* (D_5), *G. arboreum* (A_2), and *G. hirsutum* (AD_1) have been released (Paterson et al., 2012; Wang et al., 2012; Li et al., 2014, 2015; Yuan et al., 2015), which provides the foundations to understand the cotton genome organization, genetic variations, and speciation processes. Moreover, these resources facilitate functional genomic studies, which provide key information for improving the agricultural performance of cotton in the face of biotic and abiotic stresses by the manipulation of cotton genes and their regulation.

Verticillium wilt caused by *Verticillium dahliae* Kleb (*Vd*) and Fusarium wilt caused by *Fusarium oxysporum* f. sp *vasinfectum*

[1] Address correspondence to lshan@tamu.edu.
The author responsible for distribution of materials integral to the findings presented in this article in accordance with the policy described in the Instructions for Authors (www.plantcell.org) is: Libo Shan (lshan@tamu.edu).

[OPEN]Articles can be viewed without a subscription.
www.plantcell.org/cgi/doi/10.1105/tpc.19.00950

(*Fov*) are among the destructive cotton vascular diseases faced by growers. Both diseases show symptoms such as foliar chlorosis or necrosis, premature leaf defoliation, vascular discoloration, plant stunting, and wilt (Li et al., 2017b; Cox et al., 2019). Due to the vitality of resting spores and overwintering structures produced by *Fov* (chlamydospores) and *Vd* (microsclerotia), they are notoriously difficult to eradicate from infected fields (Wheeler et al., 2012; Cox et al., 2019). Currently, the development and application of disease-resistant cultivars are among the effective means to control these pathogen threats (Cianchetta and Davis, 2015; Sanogo and Zhang, 2016). The biosynthesis of phenylpropanoids, terpenoids, and reactive oxygen species (ROS), along with the salicylic and jasmonic acid signaling pathways, contribute to cotton defense against *Vd* (Gao et al., 2013a; Ashraf et al., 2018; Hu et al., 2018). *Vd* and *Fov* infection likely share overlapping and distinct features, but the molecular mechanisms of *Fov* infection and the determinants of *Fov* resistance in cotton remain largely elusive.

At the cellular level, the first line of plant innate immunity, known as pattern-triggered immunity (PTI), is elicited through perception of microbe-associated molecular patterns (MAMPs) by plant cell surface-resident pattern recognition receptors (Yu et al., 2017). Several pattern recognition receptors have been identified as receptor-like kinases (RLKs) or receptor-like proteins (RLPs; Böhm et al., 2014; Couto and Zipfel, 2016). Both RLKs and RLPs contain an extracellular domain and a single transmembrane domain, but RLPs lack the cytoplasmic kinase domain found in RLKs (Shiu and Bleecker, 2003; Jamieson et al., 2018). The extracellular domains vary in RLKs and RLPs, including the leucine-rich repeat (LRR), the lectin motif, the lysin motif (LysM), and the epidermal growth factor (EGF)-like motif (Böhm et al., 2014; Couto and Zipfel, 2016).

Emerging evidence has suggested that RLKs and RLPs play an essential role in resistance to Verticillium and Fusarium wilt diseases in a range of plant species. The most common extracellular domain of RLKs and RLPs is LRR. The tomato (*Solanum lycopersicum*) LRR-RLP Ve1 confers race-specific resistance to *Vd* carrying Ave1 (Kawchuk et al., 2001). Ve1 homologs in cotton play a role in Verticillium wilt resistance to certain isolates (Gao et al., 2011; Zhang et al., 2012). Further, in tomato, Ve1 mediates resistance to *F. oxysporum* f. sp *lycopersici* carrying Ave1 (de Jonge et al., 2012). LRR-RLPs I-1 and I-7 confer resistance to *F. oxysporum* f. sp *lycopersici* in tomato (Huang et al., 1997; Houterman et al., 2008; Gonzalez-Cendales et al., 2016).

LysM-containing RLKs and RLPs are important players during plant-fungal interactions by mediating chitin recognition and signaling activation (Wan et al., 2008; Tanaka et al., 2013; Gong et al., 2020). Chitin, the polymer of β-1,4-linked *N*-acetylglucosamine, is a component of the fungal cell wall and known as a potent MAMP in many plant species. In rice (*Oryza sativa*), OsCEBiP, an LysM-RLP, functions as a high-affinity chitin binding receptor and homodimerizes to sandwich chitin in a receptor complex at the plasma membrane (Kaku et al., 2006; Hayafune et al., 2014). OsCERK1, a LysM-RLK, which lacks chitin binding activity, associates with OsCEBiP and is essential for signaling activation (Shimizu et al., 2010). There are five *LysM-RLKs* (*LYKs*) and three *LysM-RLPs* (*LYPs*/*LYMs*) in the Arabidopsis (*Arabidopsis thaliana*) genome. AtCERK1 (AtLYK1), AtLYK4, and AtLYK5 are important for chitin perception and signaling (Miya et al., 2007; Liu et al., 2012; Wan et al., 2012; Cao et al., 2014). AtLYK5 possesses higher binding affinity to chitin than AtCERK1, and chitin perception induces AtLYK4/AtLYK5-AtCERK1 complex formation and AtLYK5-mediated AtCERK1 phosphorylation (Cao et al., 2014; Xue et al., 2019). AtLYM2 regulates chitin-induced stomatal closure in Arabidopsis (Faulkner et al., 2013). Distinct chitin perception and signaling systems exist in Arabidopsis and rice (Wan et al., 2012; Kawasaki et al., 2017).

Wall-associated kinases (WAKs) are a unique group of RLKs with extracellular EGF motifs, which likely link to the cell wall through the homogalacturonan binding domain (Decreux et al., 2006; Kanneganti and Gupta, 2008). The five Arabidopsis *AtWAKs* are clustered in a 30-kb locus on chromosome 1 with high sequence similarity (>85% identical for the kinase domains; He et al., 1999). AtWAKs are involved in cell expansion during plant development (Wagner and Kohorn, 2001). AtWAK1 was shown to bind to both long pectin molecules resident in native cell walls and short oligogalacturonic acid fragments released during pathogen infection or wounding in vitro (Decreux and Messiaen, 2005). Similarly, AtWAK2 is able to bind to the de-esterified charged galacturonic acid backbone common to pectin (Kohorn et al., 2009). Besides, AtWAK1 was proposed to be a receptor of oligogalacturonides (OGs), which are released from the plant cell wall during pathogen infections and is required for the resistance to *Botrytis cinerea* (Brutus et al., 2010). In recent years, several independent studies have highlighted the importance of the *WAK* gene family in resistance against pathogen infections in crops. Two *WAK* genes from maize (*Zea mays*) were discovered as quantitative resistance loci important for resistance against northern maize leaf blight and head smut (Hurni et al., 2015; Zuo et al., 2015; Yang et al., 2019). The disease resistance gene *Xanthomonas oryzae* pv *oryzae* resistance 4 in rice encodes a WAK that promotes cellulose synthesis and strengthens the plant cell wall, thereby enhancing plant resistance against both bacterial (*X. oryzae* pv *oryzae*) infection and lodging (Hu et al., 2017). SlWAK1 from tomato promotes the apoplast immunity against bacterial pathogen *Pseudomonas syringae* (Zhang et al., 2020). Besides, the Arabidopsis genome contains 21 *WAK-like* (*WAKLs*) genes (Verica and He, 2002; Verica et al., 2003), some of which play a role in plant disease resistance. For example, Arabidopsis WAKL RFO1, and LRR-RLP RFO2 confer quantitative resistance to a broad spectrum of different *Fusarium* races, suggesting that a common elicitor or MAMP in *Fusarium* might contribute to the resistance (Diener and Ausubel, 2005; Shen and Diener, 2013). Thus, both WAK and LYK family genes are important regulators in plant resistance against different fungal pathogens.

To test whether the WAK and LYK family genes play a role in cotton fungal disease resistance, we performed a genome-wide identification of cotton WAK and LYK family genes in silico and identified 13 *GhWAK* and 17 *GhLYK* genes in *G. hirsutum*. The phylogenetic analysis unraveled the evolutionary conservation of LYKs, and the interspecies divergence of WAKs between cotton and Arabidopsis. Together with RNA sequencing (RNA-seq), loss-of-function screens using Agrobacterium (*Agrobacterium tumefaciens*) mediated virus-induced gene silencing (VIGS) and biochemical assays, GhWAK7A, GhCERK1, and GhLYK5 were demonstrated to contribute to cotton resistance to *Fov* and *Vd* and

mediate chitin perception and signaling in cotton. GhWAK7A phosphorylates GhLYK5 and regulates chitin-induced GhCERK1 and GhLYK5 association. Our results reveal that a wall-associated RLK, GhWAK7A, functions in cotton fungal disease resistance via the modulation of chitin signaling.

RESULTS

Identification of *WAK* Family Genes in Cotton

WAKs represent a class of RLKs characterized by an aminol (N)-terminal conserved signal peptide, an extracellular WAK galacturonan binding domain, an EGF-like domain, an EGF calcium binding (EGF-Ca^{2+}) domain, a transmembrane domain, and a carboxyl (C)-terminal cytosolic Ser/Thr protein kinase domain (Verica and He, 2002). The Arabidopsis genome encodes five *WAKs* and 21 *WAKL* genes, which bear different extracellular domain configurations and show only 18% to 22% identities in their extracellular regions to *WAKs* (Verica et al., 2003). Our study here is mainly focused on the genome-wide identification of cotton *WAK* genes. Using five Arabidopsis AtWAK proteins as queries, we performed a genome-wide identification of cotton *WAK* genes in the genome database of representative cotton species including an allotetraploid cotton (*G. hirsutum*) and two diploid cotton species (*G. arboreum* and *G. raimondii*). The databases used in this study included the Nanjing Agricultural University (NAU) assembly for *G. hirsutum* (Zhang et al., 2015), the Joint Genome Institute (JGI) assembly for *G. raimondii* (Paterson et al., 2012), and the Cotton Research Institute (CRI) assembly for *G. arboreum* (Li et al., 2014).

To identify *WAK* genes in these cotton species, we implemented a pipeline wherein BLASTp (https://cottonfgd.org/blast/) search results were refined manually by evaluating protein domain predictions for subject amino acid sequences (Figure 1A). First, the full-length amino acid sequences of five AtWAKs were used as the queries for the BLASTp search against the three cotton genome databases *G. hirsutum* (AD_1)-NAU, *G. raimondii* (D_5)-JGI, and *G. arboreum* (A_2)-CRI, with a threshold of E-value < 1e-50. Second, proteins annotated as non-WAK proteins or WAKL proteins were removed from the list. Furthermore, we verified the presence of the conserved abovementioned various WAK domains of candidates. The domain prediction was performed using the protein sequence analysis tools from the programs SMART (http://smart.embl-heidelberg.de/) and Interpro (https://www.ebi.ac.uk/interpro/). Proteins, which lack essential domains of WAKs, were eliminated from the data set. After manually evaluating the protein predictions of each candidate, we identified 13 putative *GhWAKs* from the *G. hirsutum* (Supplemental Table 1), 16 *GaWAKs* from the *G. arboreum* (Supplemental Table 2), and 11 *GrWAKs* from the *G. raimondii* (Supplemental Table 3). *G. arboreum* has more *WAK* members than *G. hirsutum*, suggesting massive gene deletions during tetraploid *G. hirsutum* speciation (see below for examples). The phylogenic analysis of these candidates with AtWAKs and AtWAKLs revealed that they are phylogenetically closer to AtWAKs than AtWAKLs, indicating that the cotton proteins we identified here are WAKs, but not WAKLs (Supplemental Figure 1).

Phylogenetic Analysis and Evolution of *WAK* Family Genes in Cotton

To elucidate the evolutionary relationship of WAK family proteins in Arabidopsis and cotton, we performed a phylogenetic analysis of cotton and Arabidopsis WAK proteins using the tool MEGA X (Kumar et al., 2018). No cotton WAKs from *G. hirsutum*, *G. arboreum*, and *G. raimondii* were found to interleave with the isolated clade formed by the five Arabidopsis AtWAKs (Supplemental Figure 2). This result remains consistent when the WAKs from *G. hirsutum*, *G. arboreum*, or *G. raimondii* database were analyzed separately (Figure 1B and Supplemental Figures 3A and 3B). The phylogeny using the kinase domains also indicated that WAKs from different cotton species form a separate clade from AtWAKs (Supplemental Figure 4). The five AtWAK proteins share 60% to 80% identities while the identities among AtWAK and GhWAK proteins are 30% to 50% (Supplemental Table 4). Collectively, this suggests that members of WAKs in cotton and Arabidopsis have likely evolved independently. Based on the phylogenetic relationships, we divided the cotton WAK members into five clades (I to V) with GhWAK1D, GhWAK2D, and GhWAK3D in clade I; GhWAK4D in clade II; GhWAK5A and GhWAK5D in clade III; GhWAK6D, GhWAK7A, GhWAK8A, and GhWAK8D in clade IV; and GhWAK9D, GhWAK10A, and GhWAK10D in clade V in *G. hirsutum* (Figure 1B; Supplemental Figure 2; Supplemental Table 5). Because this study is focused on GhWAKs, we named the individual members of WAKs from *G. hirsutum*. In consideration of the allotetraploid nature of *G. hirsutum* (AADD), the names of GhWAKs were followed with an uppercase "A" or "D" indicating the gene derived from the A- or D-subgenome (Figure 1B; Supplemental Table 6). For the homoeologous genes in A- and D-subgenomes, we gave the same name followed by an "A" or "D," such as GhWAK10A and GhWAK10D.

Among 13 GhWAKs, nine are in the D-subgenome and four are in the A-subgenome (Figure 1C). The phylogenic analysis showed all the four *GhWAK* genes from the A-subgenome are orthologous to genes from the *G. arboreum* genome (Supplemental Figures 5A and 6) and three of them have corresponding D-subgenome homeologs (Figure 1B; Supplemental Figure 6). Interestingly, three *GhWAKs* (*GhWAK7A*, *GhWAK8A*, and *GhWAK10A*) on chromosome 2 of *G. hirsutum* A-subgenome are orthologous to WAKs on chromosome 3 of *G. arboreum* A-genome (Figure 1C; Supplemental Figure 5A), which may be due to the reciprocal translocation during the speciation of tetraploid *G. hirsutum* (Hu et al., 2019). Apparently, 12 out of 16 *GhWAKs* from *G. arboreum* were lost during *G. hirsutum* speciation (Supplemental Figures 5A and 6). Of the nine *GhWAKs* from the D-subgenome, seven genes have corresponding orthologs from *G. raimondii* (Supplemental Figures 5B and 6). Two other genes, *GhWAK1D* and *GhWAK3D*, are tandemly arranged and share high protein identity with *GhWAK2D* (92% and 87% respectively; Figure 1C; Supplemental Table 4), indicating they might have recently evolved as a result of tandem gene duplication in *G. hirsutum*. One pair of orthologs in *G. raimondii* and *G. arboreum* (Ga03G0824.1; Gorai.005G086200.1) do not have associated *G. hirsutum* counterparts (Supplemental Figure 6), suggesting that either the *G. hirsutum* ortholog was lost during the speciation, or the *G. hirsutum* ortholog was not able to be resolved with the genome assembly used in this study.

We attempted to further understand how *WAK* genes have evolved in cotton by comparing the number and relatedness of WAKs in *A. thaliana*, *G. arboreum*, *G. raimondii*, and *G. hirsutum*. Inferences made using the phylogenetic analysis between *GhWAKs* from the A-subgenome and *GaWAKs*, and *GhWAKs* from the D-subgenome and *GrWAKs* (Supplemental Figures 5A, 5B, and 5C, and 6), suggested that the trajectory of *WAK* gene number changes during the cotton genome evolution (Figure 1D). We propose that there might be seven *WAK* genes in the most recent common ancestor of two diploid cotton species (*G. arboreum* and *G. raimondii*) with massive gene duplications and losses during the evolution of *G. arboreum*, *G.*

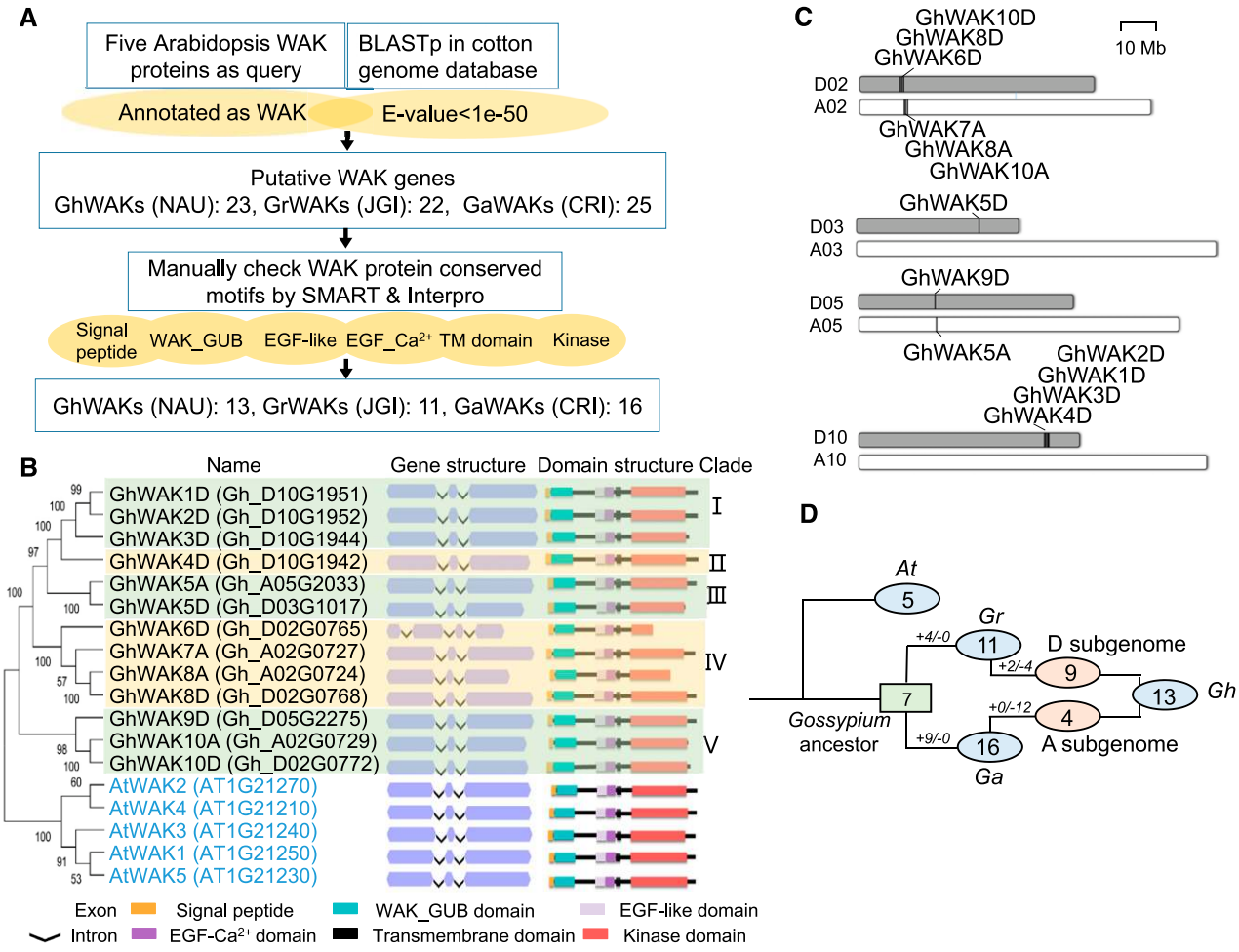

Figure 1. Identification and Phylogenetic Analysis of WAK Family Proteins in Cotton.

(A) Genome-wide identification pipeline of *WAKs* in cotton genomes. Five Arabidopsis *WAK* genes annotated in TAIR10 were used as the query sequences for a BLASTp (cutoff: E-value < 1.0e-50) against three cotton genomes. The results from this BLAST search were refined using protein domain prediction tools (e.g., SMART, InterPro) to eliminate non-WAKs by manually screening proteins without any conserved WAK motifs.

(B) A phylogenetic view of *GhWAK* family proteins, gene structures, protein motifs, and clade partitions. The five AtWAK proteins were included to depict the evolutionary distance of the WAK proteins between *G. hirsutum* and *A. thaliana*. The phylogenetic tree was generated by the neighbor-joining method with 1,000 bootstrap replicates in the program MEGA X. The five AtWAKs are shown in blue. The NAU accession ID of each *GhWAK* is labeled adjacent to the *GhWAK* name curated in this study. Gene structures are further diagrammed next to each *GhWAK* using purple boxes to indicate exons and black shrunken lines with the same length to indicate introns. Schematics depicting WAK protein motifs were manually confirmed using the tool SMART (http://smart.embl-heidelberg.de/). A legend for the protein domain schematics is included at the bottom. Alignments corresponding to these analyses can be found in Supplemental Files 1 and 2.

(C) Genomic locations of *GhWAK* genes on their corresponding chromosomes. White bars represent chromosomes from the A-subgenome of *G. hirsutum* while gray bars represent the D-subgenome chromosomes. Chromosomes that were not found to contain *WAK* genes were not included in this figure.

(D) The evolutionary trajectory of *WAK* family in *A. thaliana* (*At*), *G. arboreum* (*Ga*), *G. raimondii* (*Gr*), and *G. hirsutum* (*Gh*). Numbers in circles represent the number of family members in each genome or subgenome, and the gene number for the most recent common ancestor of two diploid cotton species is shown in rectangles. Numbers on the line connecting each node with plus (+) and minus (−) signs indicate the numbers of duplicated and deleted genes, respectively.

raimondii, and *G. hirsutum* (Figure 1D; Supplemental Figure 5C).

The chromosomal distribution of *AtWAK* genes indicates a tandemly arrayed gene (TAG) cluster on chromosome 1 (He et al., 1999). We investigated the physical positions of *GhWAK* genes in the *G. hirsutum* genome and found that *GhWAKs* distribute unevenly among six chromosomes with many members as TAG clusters (Figure 1C). *GhWAK1D*, *GhWAK2D*, *GhWAK3D*, and *GhWAK4D* present as a cluster of TAGs on the D10 chromosome. Notably, *GhWAK1D*, *GhWAK2D*, *GhWAK3D*, and *GhWAK4D* are clustered together on the phylogenetic tree with 83% to 93% identities between each other, suggesting these four paralogous *GhWAKs* likely were derived from one ancestor. Surprisingly, there are no corresponding homoeologous genes of these four GhWAKs on the A subgenome (Figure 1C). However, there are seven *GaWAKs* as a cluster of TAGs on chromosome 10 of *G. arboreum* (A-genome ancestor; Supplemental Figure 5A), suggesting that this cluster was lost during speciation of tetraploid *G. hirsutum*.

The other two separate clusters are composed of *GhWAK6D*, *GhWAK8D*, and *GhWAK10D* on the D02 chromosome and *GhWAK7A*, *GhWAK8A*, and *GhWAK10A* on the A02 chromosome. *GhWAK8A-GhWAK8D* and *GhWAK10A-GhWAK10D* are likely two pairs of positional homeologs with 89.46%% and 94.33% protein identities, respectively (Figure 1C). *GhWAK6D* and *GhWAK7A* are also possible homoeologous genes with relatively high divergence (63.11% protein identity). Thus, they were given different names.

Interestingly, the closest orthologs of *GhWAK1D*, *GhWAK2D*, *GhWAK3D*, and *GhWAK4D* in *G. raimondii* (D-genome ancestor) are *Gorai.011G218500* and *Gorai.011G218100*, two TAGs on chromosome 11 (Supplemental Figure 5B), in accordance with the observation that the D-subgenome chromosome 10 of *G. hirsutum* has a high collinear relationship with the D-genome chromosome 11 of *G. raimondii* (Hu et al., 2019). The orthologs of *GhWAK7A*, *GhWAK8A*, and *GhWAK10A* in *G. arboreum* are *Ga03G0825.1*, *Ga03G0822.1*, and *Ga03G0831.1*, three TAGs on chromosome 3, respectively (Supplemental Figure 5A). Regarding the collinear relationship between *G. hirsutum* A-subgenome chromosome 2 and *G. arboreum* chromosomes 2 and 3 (Hu et al., 2019), we infer these three genes (*GhWAK7A*, *GhWAK8A*, and *GhWAK10A*) were translocated from chromosome A02 to A03 during the speciation of *G. hirsutum*. Together, these analyses indicate that *WAKs* are highly evolved genes with extensive gene duplications, losses, and translocations.

Next, we analyzed the gene and protein domain structures of *GhWAKs* and *AtWAKs*. Like their Arabidopsis orthologs, most *GhWAKs* contain three exons and two introns, except *GhWAK6D*, which contains four exons and three introns (Figure 1B). The six motifs, including the signal peptide, and GUB_WAK, EGF_like, EGF_Ca^{2+}, transmembrane region, and the kinase domain, are conserved and common to both GhWAKs and AtWAKs (Figure 1B). Alignments of the amino acid frequencies of the EGF_like domains in GhWAKs revealed six highly conserved Cys residues (x**C**xxxxxxxxxx**C**xxxSx**C**xxxxxxxGYx**C**K**C**xxGxxGxxGxPYxxxG**C**x, where *x* is any amino acid; Supplemental Figure 7A), which are implicated in the formation of disulfide bonds (Appella et al., 1988). A similar analysis of GhWAK EGF_Ca^{2+} domains revealed the expected conservation of five amino acid residues (**D**x**D/NE**CxxxxxxxCxxxxxCx**N**xxGx**Y**xCxCxxxxxGDxxxxxxGCx) required for calcium binding (Rao et al., 1995; Supplemental Figure 7B). The WAK domain is the most variable of all the domains contained within a WAK protein; however, our results indicated several conserved or semi-conserved residues near the N- and C-terminal ends (N terminus: xxxCxxxCGxxxlPVPFGxxxxxCxxxxxFxIxCxxxxxxPx; C terminus: xNKFxAxGCDT) of this domain in GhWAK proteins (Supplemental Figure 7C).

GhWAK7A Is Involved in Cotton Resistance Against Fungal Wilt Pathogens

WAK family proteins have been recognized to play an important role in disease resistance against fungal pathogens by several independent studies (Zuo et al., 2015; Shi et al., 2016; Hu et al., 2017; Saintenac et al., 2018; Yang et al., 2019). To unravel the potential involvement of *GhWAKs* in response to cotton fungal pathogens, the transcriptional changes of *GhWAK* genes upon fungal pathogen infection were investigated. We first analyzed the published RNA-seq data sets from the cotton *G. hirsutum* 'YZ-1', which has been widely used for cotton transformation and regeneration, infected with the *Vd* V991 isolate prevalently present in China (Zhang et al., 2018). This analysis revealed that eight out of 13 *GhWAKs* were upregulated at 6-, 12-, or 24-h post-inoculation (hpi), with *GhWAK7A* showing 12-fold induction at 6 hpi (Figure 2A).

We then confirmed the transcriptional changes of *GhWAK* genes using reverse transcription- quantitative PCR (RT-qPCR) with gene-specific primers in *G. hirsutum* 'CA4002', a U.S. cultivar, infected by the *Vd* 'King' isolate, a prevalent field isolate in Texas, USA. In addition to *GhWAK7A*, *GhWAK5A*—which shares a relatively high protein identity (61.16%) with *GhWAK7A*, but displayed no induction within 24 hpi—was selected for comparison. Consistent with the RNA-seq result, *GhWAK7A* showed enhanced expression at 1-d post-inoculation (dpi), whereas *GhWAK5A* was only induced at 7 dpi (Figure 2B).

The transcriptional changes of *GhWAK5A* and *GhWAK7A* in response to *Vd* infections prompted us to examine their functional involvement in cotton defense against fungal diseases. We silenced the individual members of *GhWAK5A* and *GhWAK7A* by VIGS. Three weeks after Agrobacterium infiltration, RT-PCR analysis confirmed the reduced transcripts of *GhWAK* genes in the true leaves of cognate VIGS plants compared with the control vector-inoculated plants (VIGS-Ctrl; Figure 2C). In addition, RT-qPCR was performed to examine the transcript levels of individual *GhWAK* homologs in roots, where vascular pathogens first infect the plant. The results showed that the transcripts of *GhWAK7A* and *GhWAK5A*, but not any of the other eight *GhWAK* homologs, were reduced in the cognate VIGS plants compared with the control plants (Figure 2D), confirming the efficiency and specificity of VIGS silencing in cotton roots.

Three weeks after VIGS, the plants were inoculated with spores of the *Vd* 'King' isolate by a root-dipping method (Gao et al., 2013a). Compared with control, *GhWAK7A*-silenced plants displayed more wilting and yellow leaves, and deeper vascular discoloration in stem tissues (Figure 2E). We quantified the disease severity with disease index (DI) via five scales of foliar

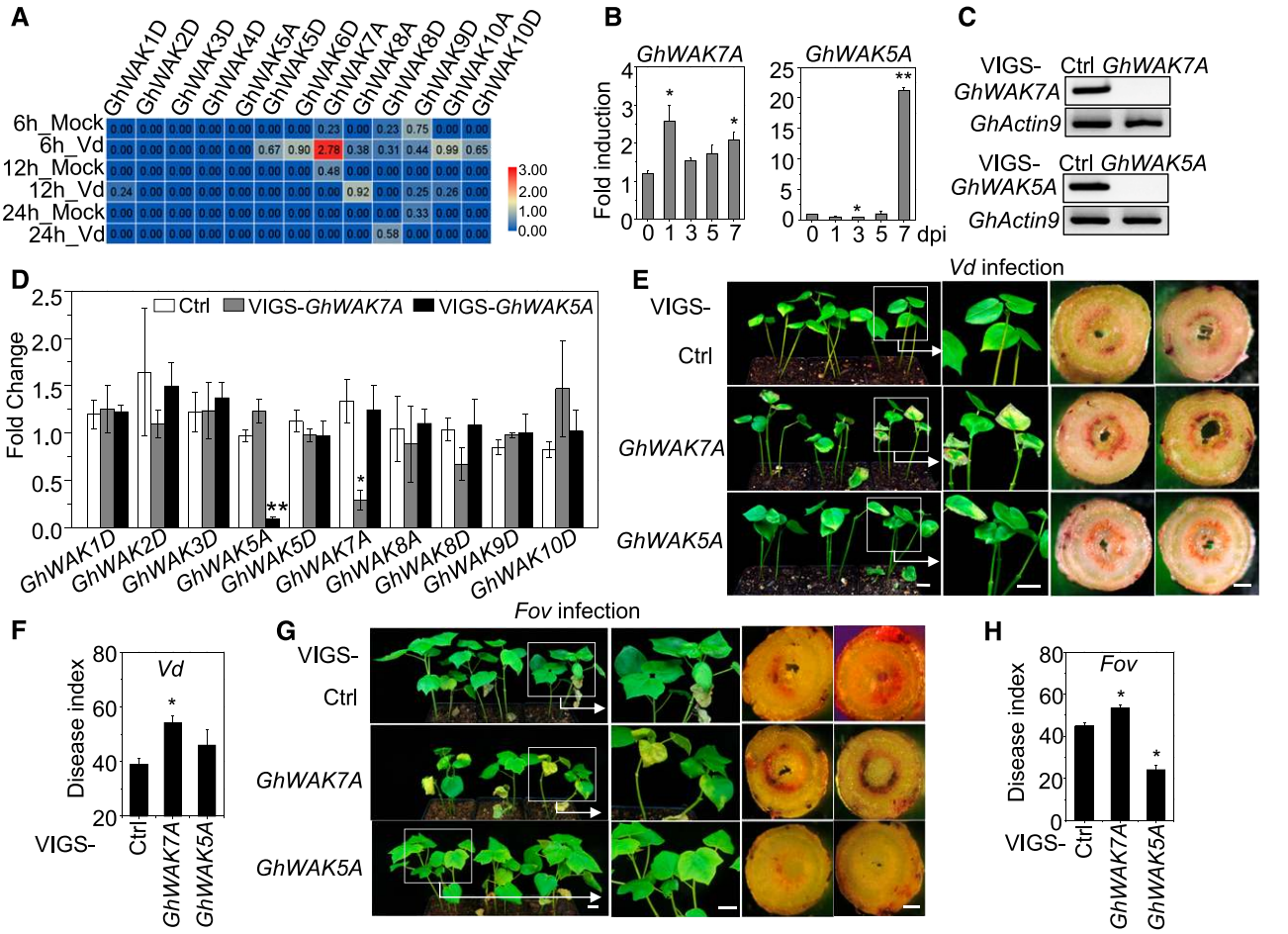

Figure 2. *GhWAK7A* Is Involved in Cotton Defense Responses against Fungal Wilt Diseases.

(A) Heat map of *GhWAK* family genes in RNA-seq data derived from cotton roots infected with the *Vd* V991 isolate (Zhang et al., 2018). The map was generated using the program Morpheus (https://software.broadinstitute.org/morpheus). Red color indicates relatively high expression and blue indicates relatively low expression. The corresponding value of fragments per kilobase of transcript per million is shown in the colored box.

(B) The expression patterns of *GhWAK5A* and *GhWAK7A* upon *Vd* infection. Two-week-old cotton seedlings were inoculated with the *Vd* 'King' isolate using a root-dipping method. The root samples were harvested at the indicated time-points for RT-qPCR. *GhUBQ1* was used as an internal control. The data are shown as mean ± SE from three independent repeats. Asterisks indicate a significant difference using one-way ANOVA (*P < 0.05; **P < 0.01).

(C) Expression of *GhWAK* genes in control and silenced plants measured by RT-PCR. Cotyledons from 2-week-old cotton were syringe-infiltrated with Agrobacterium carrying a VIGS construct to silence *GhWAK7A* (VIGS-*GhWAK7A*), *GhWAK5A* (VIGS-*GhWAK5A*), or a GFP vector control (Ctrl). Three weeks after VIGS, the second true leaves were harvested for RNA isolation. *GhActin9* was used as an internal control.

(D) The VIGS efficiency and specificity of *GhWAK7A* and *GhWAK5A* in cotton roots by RT-qPCR analysis. Three weeks after VIGS infiltration, cotton roots were harvested for RNA isolation and RT-qPCR analysis. *GhUBQ1* was used as an internal control. Data are shown as mean ± SE from three independent repeats. Asterisks indicate significant differences from Ctrl using a two-tailed Student's *t* test (*P < 0.05; **P < 0.01).

(E) Disease symptoms of leaves and stems in *Vd*-infected VIGS-*GhWAK* genes and control plants. Three weeks after VIGS, plants were inoculated with *Vd* 'King' isolate at an inoculum of 1×10^6 spores/mL using the root-dipping method. Images depicting the severity of plant wilting were taken at 14 dpi (left representation). Close-up views from the left representations are shown in the middle. Scale bar = 2 cm for plants. Vascular discoloration was observed in the stem 1.5 cm above the soil-line at 16 dpi under an optical microscope (right representation). Scale bar = 0.5 mm for stems.

(F) The DIs after *Vd* infection. The data are shown as the mean ± SE from three independent repeats. An asterisk indicates a significant difference using one-way ANOVA (*P < 0.05).

(G) Disease symptoms of leaves and stems in *Fov*-infected VIGS-*GhWAK* genes and control plants. Three weeks after VIGS, plants were inoculated with *Fov* 'CA10' at 1×10^7 spores/mL using the root-dipping method. Images depicting the severity of foliar and plant wilting symptoms were taken at 20 dpi (left representation). Close-up views from the left representations are shown in the middle. Scale bar = 2 cm for plants. Vascular discoloration was observed in the stem, 1.5 cm above the soil-line, at 22 dpi (right representation). Scale bar = 0.5 mm for stems.

(H) The DIs after *Fov* infection. The data are shown as the mean ± SE from three independent repeats. An asterisk indicates a significant difference using one-way ANOVA (*P < 0.05).

The above experiments were repeated at least three times with similar results.

symptoms (Xu et al., 2012). Quantification of DI further supported this conclusion (Figure 2F).

We next tested whether *GhWAK7A* and *GhWAK5A* contribute to cotton defense against another fungal wilt pathogen, *Fov*, which causes Fusarium wilt. Interestingly, VIGS-*GhWAK7A* plants became more susceptible to the *Fov* CA10 isolate with more wilting leaves and plants and darker vascular discoloration in stem tissues compared with control vector-inoculated plants (Figure 2G), whereas VIGS-*GhWAK5A* plants were more resistant to the *Fov* CA10 infection with fewer wilting leaves and less vascular discoloration compared with control plants (Figure 2G). The DI also indicated that VIGS-*GhWAK7A* plants were more susceptible, while VIGS-*GhWAK5A* plants were more resistant to the *Fov* CA10 infection than the control plants (Figure 2H).

Several *WAKs* and *WAKLs* have been reported to link to plant responses against abiotic stresses (Hou et al., 2005; Xia et al., 2018; Wang et al., 2019). However, VIGS-*GhWAK7A* plants showed comparable responses to VIGS-Ctrl plants during water-deprivation and 200 mM of NaCl salt treatment (Supplemental Figure 8). Taken together, the data indicate that GhWAK7A may not be involved in cotton tolerance to drought or salt stresses but plays a positive role in cotton resistance to both *Vd* and *Fov*, implying a potentially conserved mechanism in cotton responses to different fungal pathogens.

GhWAK7A Contributes to Chitin-Induced Immune Responses in Cotton

Chitin, a conserved fungal cell wall component, triggers immune responses in plants (Shinya et al., 2015; Kawasaki et al., 2017). The contribution of *GhWAK7A* to defense against two different fungal pathogens prompted us to test the involvement of GhWAK7A in chitin-induced immune responses. RT-qPCR analysis indicated that *GhWAK7A*, but not *GhWAK5A*, was induced as early as 0.5 h upon chitin treatment (Figure 3A).

The activation of mitogen-activated protein kinases (MAPKs) is one of the early immune responses triggered by the perception of chitin and other MAMPs (Yu et al., 2017). Chitin treatment induced rapid and transient activation of GhMPK3 and GhMPK6 in cotton detected by immunoblots using an anti-phosphorylated extracellular-regulated protein kinase 1/2 antibody (Supplemental Figure 9A). The activation of GhMPK3 and GhMPK6 was confirmed using VIGS-*GhMPK3* or VIGS-*GhMPK6* plants in which the protein levels of GhMPK3 or GhMPK6 were reduced (Supplemental Figures 9A and 9B). Compared with control, the silencing of *GhWAK7A*, but not *GhWAK5A*, resulted in compromised GhMPK6 and GhMPK3 activation without affecting the GhMPK6 or GhMPK3 protein levels (Figures 3B and 3C).

The production of ROS is another well-characterized immune response triggered by chitin and other MAMPs (Yu et al., 2017). The chitin-induced ROS production was lower in *GhWAK7A*-silenced cotton plants than that in the control plants (Figure 3D). Chitin treatment induced expression of *GhWRKY30* and *GhMPK3* in cotton, and the expression levels of both *GhWRKY30* and *GhMPK3* after chitin treatment were reduced in *GhWAK7A*-silenced cotton plants relative to control plants (Figure 3E). Collectively, these data indicate that GhWAK7A is involved in the chitin-induced immune responses.

Earlier studies suggested that AtWAKs bind pectin in plant cell walls and are involved in cell expansion during development and the responses to pathogens and wounding (Brutus et al., 2010; Kohorn, 2016; Riese et al., 2018). To examine whether the sensing of cell-wall–derived pectin may account for the role of GhWAK7A and GhWAK5A in defense responses, we examined MAPK activation triggered by OGs, pectin fragments derived from the partial hydrolysis of plant cell wall pectin (Galletti et al., 2009). OGs were generated by the digestion of polygalacturonic acid (Na^+ salt) with *Aspergillus niger* endopolygalacturonase. The RT-qPCR data showed that the induction of *AtFRK1* by OGs was similar to that by flg22 in Arabidopsis (Supplemental Figure 10A). High-performance anion-exchange chromatography with pulsed amperometric detection indicated OG oligomers with a distribution of the degree of polymerization between 6 and 20 and an enrichment in the degree of polarization around 12 (Supplemental Figure 10B). This is consistent with the analysis using electrospray ionization mass spectrometry (Supplemental Figure 10C). Cotton leaves treated with OGs triggered rapid GhMPK6 and GhMPK3 activation with a peak at 15 min (Supplemental Figure 10D), and ROS production (Supplemental Figure 10E) and transcriptional upregulation of *GhWRKY30* and *GhMPK3* at 30 min in cotton (Supplemental Figure 10F).

However, compared with control plants, the silencing of *GhWAK7A* did not affect OG-induced MAPK activation (Figure 3F), ROS production (Figure 3G), and *GhWRKY30* and *GhMPK3* upregulation (Figure 3H). In addition, the fungal cell wall extracts from *Fov* 'CA10' (FovCWE) triggered immune responses, including MAPK activation. However, compared with control plants, the silencing of *GhWAK7A* or *GhWAK5A* did not affect FovCWE-induced MAPK activation (Figure 3I). This contrasts with the requirement of GhWAK7A in chitin-induced immune responses, suggesting that the function of GhWAK7A in plant defense might not be due to its role in response to cell-wall–derived components.

Identification and Functional Analysis of Chitin-Sensing Receptor Complex in Cotton

The Arabidopsis LYKs with the extracellular LysM motif compose a family of proteins with five members (Tanaka et al., 2013). AtCERK1 (AtLYK1), AtLYK4, and AtLYK5 were reported to function in chitin perception and signaling activation (Miya et al., 2007; Liu et al., 2012; Wan et al., 2012; Cao et al., 2014). Chitin-induced MAPK activation and ROS production were abolished in the *atcerk1* mutant and *atlyk4/5* double mutant and were reduced in the *atlyk4* mutant compared with wild-type Columbia-0 (Col-0) plants (Supplemental Figures 11A and 11B; Cao et al., 2014; Xue et al., 2019). However, the *atlyk5* (*atlyk5-2*) mutant exhibited a slight reduction in chitin-induced ROS production and no observable difference in chitin-induced MAPK activation compared with wild-type plants (Supplemental Figure 11). AtLYK4 and AtLYK5 function as the chitin receptor and AtCERK1 is likely a coreceptor or signaling partner of AtLYK4/AtLYK5 (Liu et al., 2012; Cao et al., 2014; Xue et al., 2019). We further tested whether the AtLYK4/5-AtCERK1 chitin sensory complex is involved in Arabidopsis response to *Verticillium* and *Fusarium* wilt pathogens. It has been reported that *Vd* could infect Arabidopsis (Veronese et al., 2003), and *F. oxysporum* (*Fo*) '5176' is a pathogenic fungus on

Arabidopsis (Thatcher et al., 2012). The *atcerk1* and *atlyk4/5* mutants were more susceptible to *Vd* and *Fo* '5176' infections in terms of disease symptom development (Figure 4A) and DI (Figure 4B) compared to wild-type plants. Thus, Arabidopsis AtCERK1 and AtLYK4/5 play a positive role in resistance against *Verticillium* and *Fusarium* fungal pathogens.

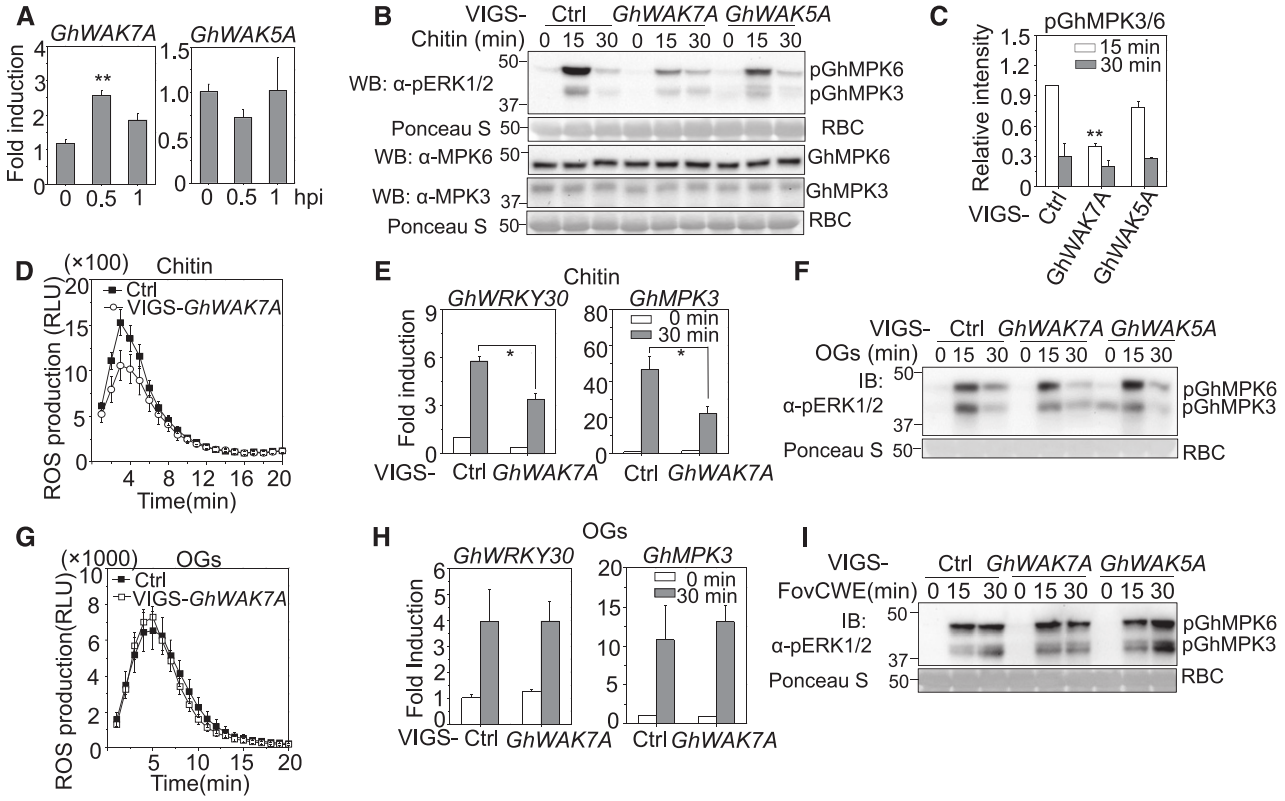

Figure 3. The Involvement of GhWAK7A in the Chitin-Triggered but Not OG-Triggered Immune Responses in Cotton.

(A) The expression pattern of *GhWAK5A* and *GhWAK7A* upon chitin treatment. The leaf discs from cotton true leaves were soaked in distilled water overnight to eliminate wounding stress and treated with 100 μg/mL of chitin solution. Samples were harvested at the indicated time-points for RT-qPCR analysis. The data are shown as mean ± SE from three independent repeats. Asterisks indicate a significant difference using a two-tailed Student's *t* test (**P < 0.01).

(B) Silencing *GhWAK7A* in cotton reduces chitin-induced MAPK activation. Cotton seedlings were silenced with *GhWAK7A*, *GhWAK5A*, or Ctrl by VIGS. The leaf discs from the second pair of true leaves were treated with 100 μg/mL of chitin at the indicated time-points. Phosphorylated GhMPK3 (pGhMPK3) and GhMPK6 (pGhMPK6) were detected by immunoblotting with an anti-phosphorylated extracellular-regulated protein kinase 1/2 (α-pERK1/2) antibody. The protein levels of GhMPK6 and GhMPK3 were detected with α-MPK6 and α-MPK3 antibodies, respectively. Protein loading is indicated by Ponceau S staining for Rubisco (RBC). The molecular mass (kDa) was labeled on the left of images (same for other immunoblots).

(C) The quantification of the relative intensities of immunoblot bands in **(B)**. The values indicate the densitometry units of phosphorylated GhMPK3/6 (pGhMPK3/6) bands normalized to the protein inputs at 15 or 30 min after chitin stimulation. The data are shown as mean ± SE from three independent repeats. Asterisks indicate a significant difference using one-way ANOVA (**P < 0.01).

(D) Silencing *GhWAK7A* in cotton dampens chitin-induced ROS production. Three weeks after VIGS, the leaf discs from the second true leaves were soaked in distilled water overnight to eliminate wounding stress and treated with 100 μg/mL of chitin. ROS production was measured at the indicated time-points. The data are shown as the mean ± SE ($n \geq 8$).

(E) Silencing *GhWAK7A* reduces chitin-induced *GhWRKY30* and *GhMPK3* expression. Three weeks after VIGS, true leaves were treated with 100 μg/mL of chitin and collected at 0 and 30 min for RT-qPCR analysis. *GhUBQ1* was used as an internal control. The data are shown as mean ± SE from three independent repeats. An asterisk indicates a significant difference using a two-tailed Student's *t* test (*P < 0.05).

(F) Silencing of *GhWAK7A* or *GhWAK5A* by VIGS does not alter OG-induced MAPK activation in cotton leaves. Three weeks after VIGS, leaf discs from the second true leaves were treated with 100 μg/mL OGs at the indicated time-points. MAPK activation assays were done as in **(B)**.

(G) Silencing *GhWAK7A* in cotton does not affect OG-induced ROS production. After VIGS infiltration, the cotton leaf discs were treated with 100 μg/mL of OGs, and ROS production was measured as described in **(D)**. The data are shown as the mean ± SE ($n \geq 8$).

(H) Silencing *GhWAK7A* in cotton does not affect OG-induced *GhWRKY30* and *GhMPK3* expression. Three weeks after VIGS, the cotton leaf discs were treated with 100 μg/mL of OGs and RT-qPCR analysis was performed as in **(E)**. The data are shown as mean ± SE from three independent repeats.

(I) Neither silencing *GhWAK7A* nor *GhWAK5A* alters FovCWE-induced MAPK activation in cotton. Three weeks after VIGS, the cotton leaf discs were treated with 1 mg/mL of FovCWE isolated from *Fov* 'CA10'. The MAPK activation was detected as in **(B)**.

The above experiments were repeated at least three times with similar results.

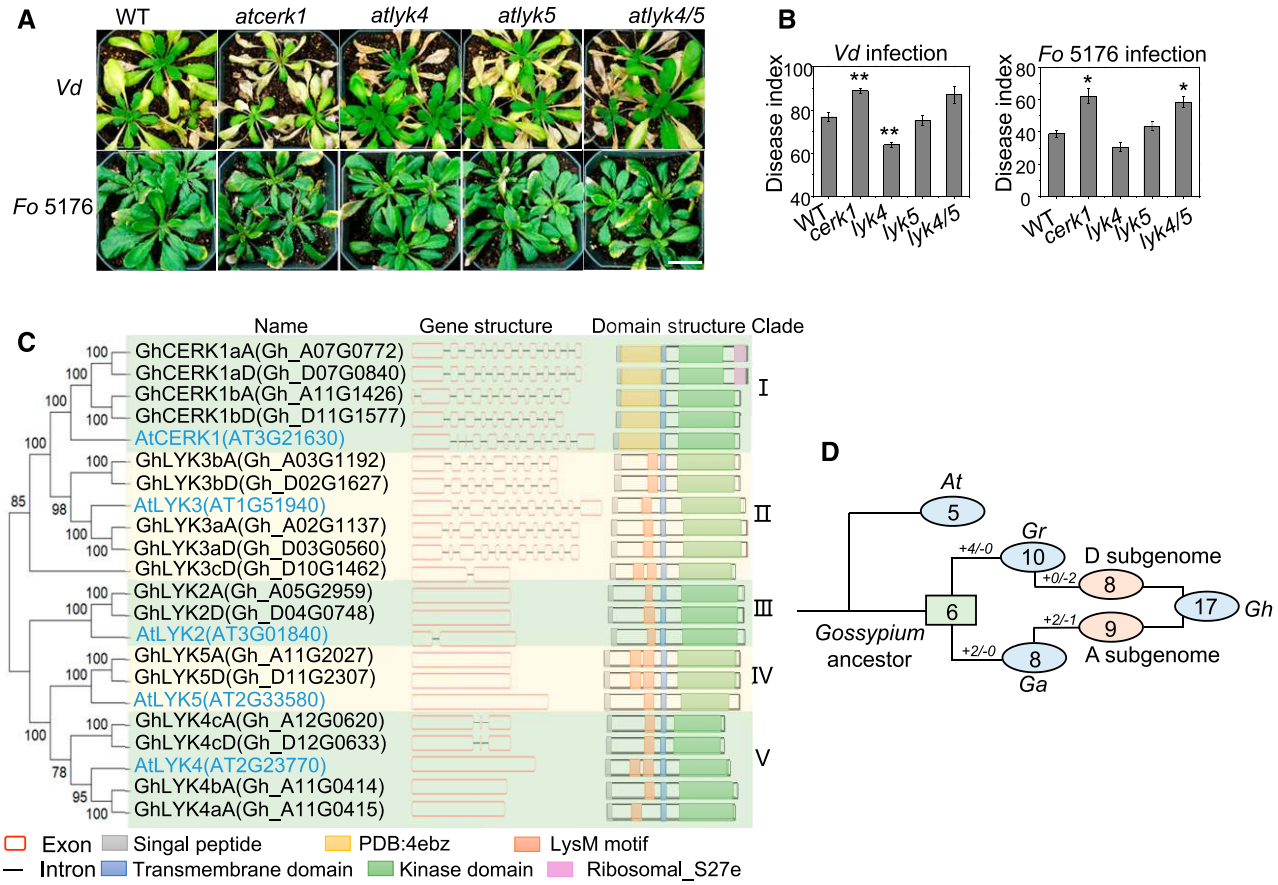

Figure 4. Arabidopsis LYKs Mediate Resistance against Fungal Wilt Diseases and Phylogenetic Analysis of Cotton *LYK* Family.

(A) *atcerk1* and *atlyk4/5* are susceptible to *Vd* and *F. oxysporum* infections. Three-week-old Arabidopsis plants were inoculated with *Vd* 'King' isolate at 1×10^6 spores/mL or *F. oxysporum* (*Fo* '5176') at 1×10^7 spores/mL via the root-dipping method. The images were taken 17 d after *Vd* infection (top) or *Fo* '5176' infection (bottom). Scale bar = 2 cm.

(B) The DIs of Arabidopsis plants infected by *Vd* and *Fo* '5176'. The DIs were calculated at 22 dpi for *Vd* infection and 20 dpi for *Fo* '5176' infection. The data are shown as mean ± SE from three independent repeats. Asterisks indicate a significant difference using one-way ANOVA (*P < 0.05; **P < 0.01). The experiments in **(A)** and **(B)** were repeated at least three times with similar results.

(C) Phylogenetic analysis of GhLYK family proteins and corresponding protein motifs. Five Arabidopsis LYK proteins were included to represent the different clades of LYK family. The phylogenetic tree was constructed as described in Figure 1B. The GhLYK name generated in this study was labeled adjacent to the gene NAU accession ID. Gene structures are diagrammed next to each GhLYK using red boxes to indicate exons and black lines with the same length to indicate introns. A schematic diagram of LYK protein motifs was constructed based on the predictions in the tool SMART. A legend for the protein motif is included at the bottom. Alignments corresponding to these analyses can be found in Supplemental Files 3 and 4.

(D) The evolutionary trajectory of *LYK* family in *A. thaliana* (*At*), *G. arboreum* (*Ga*), *G. raimondii* (*Gr*), and *G. hirsutum* (*Gh*). Numbers in circles represent the number of family members in each genome or subgenome, and the gene number for the most recent common ancestor of two diploid cotton species is shown in the rectangle. Numbers on the line connecting each node with plus (+) and minus (−) signs indicate the numbers of duplicated and deleted genes, respectively.

To uncover the chitin perception and signaling mechanism in cotton, we first performed an in silico analysis to identify the *LYK* family members in cotton using a similar method as we did for cotton *WAKs*. The Arabidopsis five LYK full-length amino acid sequences were used as BLASTp queries against three cotton databases in CottonFGD (https://cottonfgd.org/) with a threshold E-value < 1e-50. The candidates were further manually screened to retain only those proteins that contain a predicted signal peptide, LysM motif (or the extracellular CERK1 structure; Protein Data Bank [PDB] ID is PDB:4EBZ), transmembrane domain, and Ser/Thr kinase domain. Seventeen *GhLYKs* from the *G. hirsutum* genome were identified (Supplemental Table 7). Eight *GaLYKs* and 10 *GrLYKs* were identified from the genomes of *G. arboreum* and *G. raimondii*, respectively (Supplemental Tables 8 and 9).

To understand the evolutionary history of *LYK* gene family members, the 35 cotton LYKs and five Arabidopsis LYKs were subjected to a phylogenetic analysis using the program MEGA X. Interestingly, cotton LYKs can be classified into five clades with each of five Arabidopsis LYK proteins in one clade (Figure 4C, Supplemental Figure 12; Supplemental Table 10). This is different

from the phylogenetic relationship of WAKs in cotton and Arabidopsis, in which none of the Arabidopsis WAKs interleave with cotton WAKs (Supplemental Figure 2). This indicates that *LYK* members may have evolved before cotton and Arabidopsis speciation, whereas *WAKs* may have evolved independently after cotton and Arabidopsis speciation.

GhLYKs were named considering the orthology to AtLYKs and homoeology between A- and D-subgenomes (Figure 4C; Supplemental Table 11). The number (1 to 5) is to indicate the clade relativeness to the five AtLYKs (I to V). Lowercase letters (a to c) are added after the number to differentiate genes in the same clade. An uppercase "A" or "D" is followed to indicate from either the A- or D-subgenome. In *G. hirsutum*, four proteins, including GhCERK1aA, GhCERK1aD, GhCERK1bA, and GhCERK1bD, are putative AtCERK1 orthologs with 50% to 60% protein identity (Figure 4C; Supplemental Table 12). Five GhLYK3, including GhLYK3aA, GhLYK3aD, GhLYK3bA, GhLYK3bD, and GhLYK3cD, are putative orthologs of AtLYK3; and two GhLYK2—GhLYK2A and GhLYK2D—could be inferred as AtLYK2 orthologs. Four proteins with 30% to 50% identity to AtLYK4, including GhLYK4aA, GhLYK4bA, GhLYK4cA, and GhLYK4cD, and two proteins with 56% identity to AtLYK5, including GhLYK5A and GhLYK5D, are clustered (Figure 4C; Supplemental Table 12). This is consistent with the analysis in Arabidopsis that AtLYK4 and AtLYK5 have a closer evolutional relationship than the other three AtLYKs (Cao et al., 2014). The four GhCERK1 homoeologs showed an extracellular PDB:4EBZ structure (Figure 4C), which consists of three LysM motifs (Liu et al., 2012). An alignment of the GhLYK LysM motif sequences reveals four highly conserved residues (Y_D_N_P) as those in the AtLYK LysM motif (Supplemental Figures 13A and 13B). Gene structure analysis indicated that unlike *WAKs*, *CERK1* and *LYK3* in both Arabidopsis and cotton exhibit relatively complex exon–intron organization while *LYK2*, *LYK4*, and *LYK5* have no or a few introns (Figure 4C). The phylogenetic analyses also indicate that *CERK1* and *LYK3* are more closely related, whereas *LYK2*, *LYK4*, and *LYK5* are quite related in both Arabidopsis and cotton (Figure 4C).

The physical positions of *GhLYKs* distribute among eight chromosome pairs with nine genes in the A-subgenome and eight in the D-subgenome (Supplemental Figure 14). Unlike *GhWAKs* in which most of the genes are TAGs, only *GhLYK4aA* and *GhLYK4bA* are tandemly arrayed among all *GhLYKs* (Supplemental Figure 14). The phylogenetic analyses between *GhLYKs* from the A-subgenome and *GaLYKs*, and between *GhLYKs* from the D-subgenome and *GrLYKs*, suggest that seven out of nine *GhLYK* A-subgenome genes have the corresponding orthologs in *G. arboreum*, and all eight *GhLYK* D-subgenome genes have the corresponding orthologs in *G. raimondii* (Supplemental Figures 15A and 15B, and 16). The analyses revealed the trajectory of *LYK* gene number changes during the cotton genome evolution (Figure 4D). In addition, one gene (*Ga05G2087.1*) from *G. arboreum*, and two genes (*Gorai.011G012100.1* and *Gorai.006G245600.1*) from *G. raimondii*, were lost during *G. hirsutum* speciation (Supplemental Figures 15A and 15B, and 16).

There are six orthologous *LYK* genes between *G. arboreum* and *G. raimondii* (Supplemental Figure 15C), which were considered as ancestor *LYK* genes in cotton (Figure 4D). Additionally, *GhCERK1aA* and *GhLYK4bA* are unique in *G. hirsutum* (Supplemental Figure 15A). *GhLYK4bA* clusters with *GhLYK4aA* on chromosome A11 and they share a high degree of sequence identity (85.9%; Supplemental Figure 14; Supplemental Table 12), suggesting that *GhLYK4bA* may have emerged via a local duplication event from *GhLYK4aA*, which is derived from *Ga11G3609.1*. Thus, *LYKs* and *WAKs* represent two unique family genes for studying genome evolution, gene birth, death, and divergence.

Silencing *GhCERK1* or *GhLYK5* Enhances Cotton Susceptibility to Fungal Wilt Diseases

The evolutionary conservation of cotton *LYKs* and Arabidopsis *LYKs* suggests that *GhLYKs* may exhibit a function that is similar to that found in their *AtLYK* orthologs. To investigate the potential contribution of *GhLYKs* to cotton fungal diseases, we analyzed the expression pattern of *GhLYK* genes in the RNA-seq data of cotton upon infection with the *Vd* V991 isolate (Zhang et al., 2018). All the *GhLYK* genes, except *GhLYK3aD* and *GhLYK3aA*, were upregulated to different extents upon *Vd* infection at different timepoints (Figure 5A). We further deployed VIGS to silence *GhLYK1* (*GhCERK1* hereafter), *GhLYK2*, *GhLYK3*, *GhLYK4*, and *GhLYK5*. Given that there are several copies of each *GhLYK* in the cotton genome, we selected conserved regions of the given gene for VIGS and attempted to silence all the copies of the corresponding genes; for example, VIGS-*GhCERK1* would silence *GhCERK1aD*, *GhCERK1aA*, *GhCERK1bD*, and *GhCERK1bA*. Three weeks after Agrobacterium-mediated VIGS infiltration, RT-PCR analysis was performed to confirm the silencing efficiency (Figure 5B).

Compared with control plants, VIGS-*GhCERK1* plants showed markedly more severe disease symptoms that included leaf chlorosis and wilting, stem vascular discoloration (Figure 5C), and an elevated DI after *Vd* 'King' isolate infection (Figure 5D). Similar results were consistently obtained in all seven biological repeats (Supplemental Table 13). We also observed that VIGS-*GhLYK2* plants were more susceptible than control plants in five out of seven repeats, and VIGS-*GhLYK5* plants were much susceptible in four out of seven repeats relative to control plants (Supplemental Table 13). Similar to *Vd*, *Fov* CA10 infection caused more severe infection in VIGS-*GhCERK1* or VIGS-*GhLYK5* plants compared with control plants as shown with more wilting leaves and plants, darker stem discoloration, and elevated DI (Figures 5E and 5F). Among six repeats with *Fov* infections, VIGS-*GhLYK5* plants showed susceptibility in five repeats and VIGS-*GhCERK1* plants were susceptible in all repeats in terms of disease symptoms and indexes (Supplemental Table 14).

GhCERK1 and GhLYK5 Are Essential for Chitin-Triggered Immune Responses in Cotton

Given the result that *GhCERK1* and *GhLYK5* positively contribute to cotton defense against fungal wilt diseases, we further explored whether plants silenced for these genes showed altered responses to chitin treatment. Silencing of *GhCERK1* (but not *GhLYK2*, *GhLYK3*, or *GhLYK4*) compromised chitin-induced MAPK activation compared with control plants (Figures 6A and 6B). In addition, silencing of *GhLYK5* resulted in a slight, but reproducible, reduction of chitin-induced MAPK activation (Figures 6A and 6B).

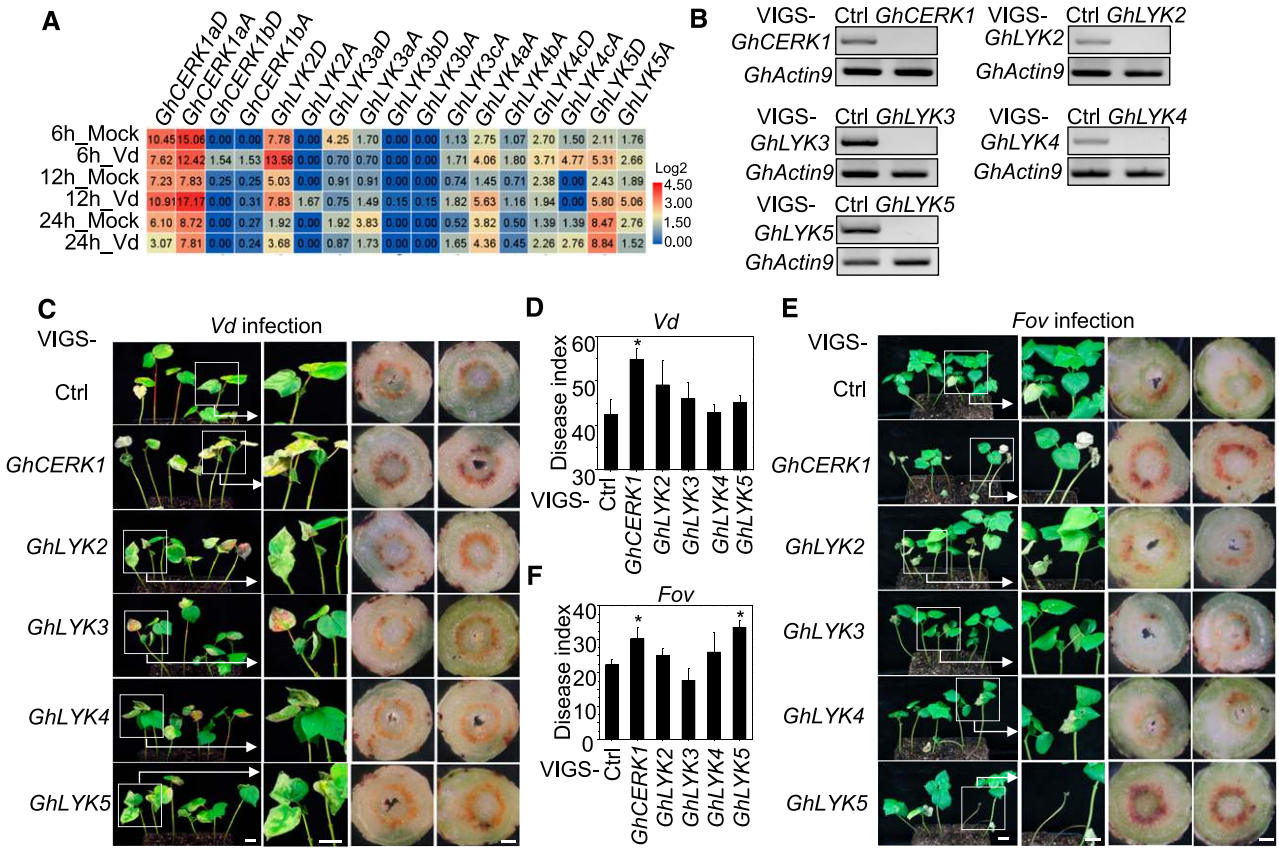

Figure 5. Silencing *GhCERK1* or *GhLYK5* Increases Cotton Susceptibility to Fungal Wilt Pathogens.

(A) Heat map of *GhLYK* family genes in RNA-seq data derived from cotton roots infected with the *Vd* V991 isolate (Zhang et al., 2018). The map was generated from the program Morpheus (https://software.broadinstitute.org/morpheus). Red color indicates the relatively high gene expression level, and blue indicates a low expression. The corresponding fragments per kilobase of transcript per million value are shown in the colored box.

(B) The expression of genes in control and silenced plants upon VIGS. Cotyledons from two-week-old cotton plants were syringe-infiltrated with Agrobacterium carrying a VIGS construct to silence *GhCERK1* (VIGS-*GhCERK1*), *GhLYK2* (VIGS-*GhLYK2*), *GhLYK3* (VIGS-*GhLYK3*), *GhLYK4* (VIGS-*GhLYK4*), *GhLYK5* (VIGS-*GhLYK5*), or a GFP control (Ctrl). The second true leaves were harvested at 3 weeks after VIGS infiltration for RNA isolation for RT-PCR analysis. *GhActin9* was used as an internal control.

(C) Cotton leaf wilting and stem vascular discoloration symptoms upon *Vd* infection. Three weeks after VIGS, plants were inoculated with the *Vd* 'King' isolate at an inoculum of 1×10^6 spores/mL using a root-dipping method. Images depicting the severity of foliar wilt symptoms were taken at 13 dpi (left). Close-up views from the left are shown in the middle. Scale bar = 2 cm for plant images. Vascular discoloration was observed in the stem, 1.5 cm above the soil-line, at 19 dpi (right). Scale bar = 0.5 mm for stem images.

(D) Quantitative measurements of disease severity after *Vd* infection. The data are shown as the mean DI ± SE from three independent repeats. An asterisk indicates a significant difference using one-way ANOVA (*$P < 0.05$).

(E) Cotton plant wilting and stem vascular discoloration upon *Fov* infection. After VIGS, plants were inoculated with *Fov* 'CA10' at 1×10^7 spores/mL using the root-dipping method. Images depicting the severity of plant wilt symptoms were taken at 20 dpi (left). Close-up views from the left are shown in the middle. Scale bar = 2 cm for plant images. Vascular discoloration was observed in the stem, 1.5 cm above the soil line at 27 dpi (right). Scale bar = 0.5 mm for stem images.

(F) Quantitative measurements of disease severity after *Fov* infection. The data are shown as mean DI ± SE from three independent repeats. An asterisk indicates a significant difference using one-way ANOVA (*$P < 0.05$).

The above experiments **(B)** to **(F)** were repeated at least three times with similar results.

Because AtLYK5 has an overlapping function with AtLYK4 in chitin perception and signaling (Cao et al., 2014), we designed a VIGS construct to silence both *GhLYK4* and *GhLYK5* simultaneously (VIGS-*GhLYK4/5*) and the VIGS efficiency was confirmed by RT-PCR (Supplemental Figure 17A). A significant reduction of chitin-induced MAPK activation was detected in VIGS-*GhLYK4/5* plants, compared with VIGS-*GhLYK4* or -*GhLYK5*, suggesting that cotton *GhLYK4* and *GhLYK5* exert redundant functions in chitin perception and signaling (Figures 6A and 6B).

Consistent with these observations, chitin-induced ROS production was largely compromised in the VIGS-*GhCERK1* or VIGS-*GhLYK4/5* plants and partially reduced in the VIGS-*GhLYK5* plants (Figure 6C). Chitin-induced marker gene expression exhibited a similar trend in these *GhLYK*-silenced cotton plants. Compared

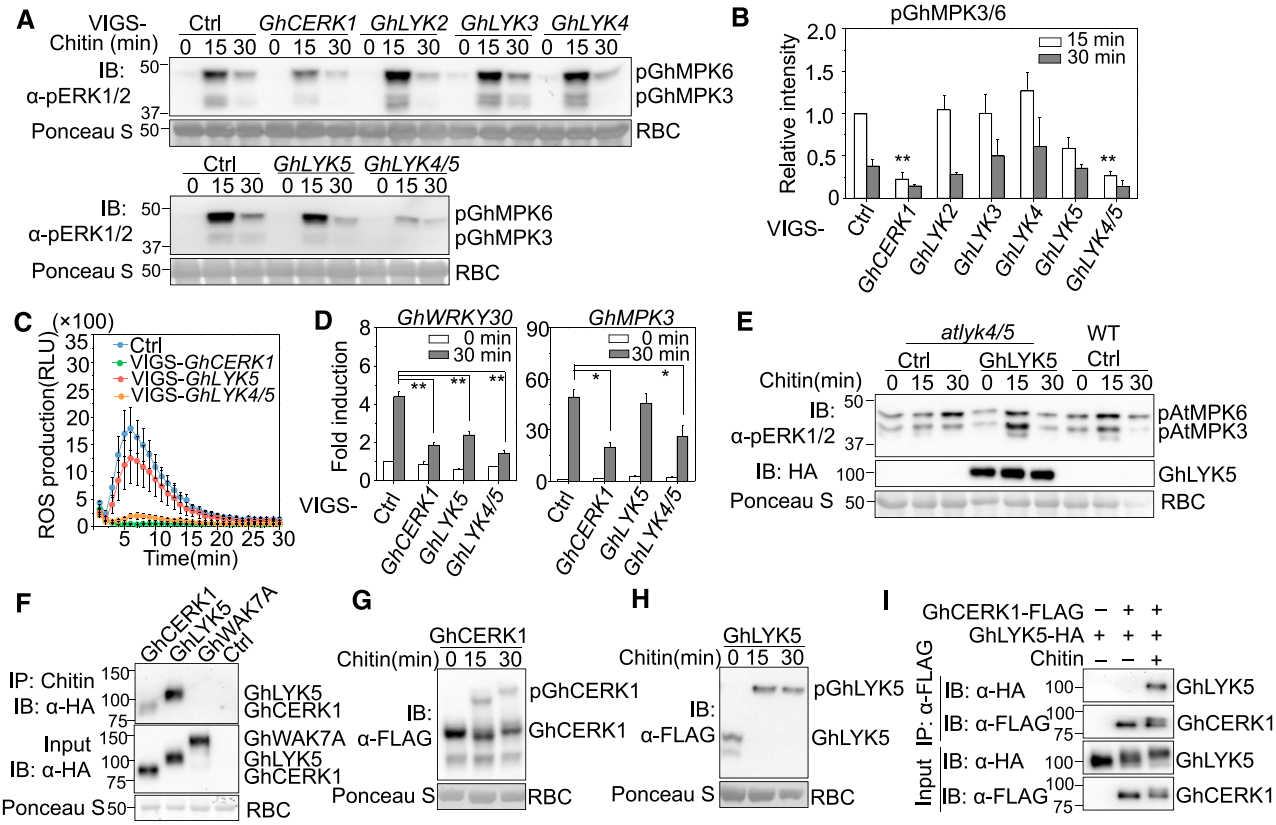

Figure 6. GhCERK1 and GhLYK5 Are Essential for Chitin Perception in Cotton.

(A) Chitin-induced MAPK activation in *GhCERK1*-, *GhLYK2*-, *GhLYK3*-, *GhLYK4*-, *GhLYK5*-, and *GhLYK4/5*-silenced cotton plants. Three weeks after VIGS, the leaf discs collected from the second true leaves were treated with 100 μg/mL of chitin at the indicated time-points for immunoblot with an α-pERK1/2 antibody. Protein loading is indicated by Ponceau S staining for RBC.

(B) The quantification of the relative intensities of immunoblot bands in **(A)**. The values indicate the densitometry units of phosphorylated MPK3/6 (pMPK3/6) bands normalized to the protein inputs at 15 or 30 min after chitin stimulation. The data are shown as mean ± SE from three independent repeats. Asterisks indicate a significant difference using one-way ANOVA (**P < 0.01).

(C) Chitin-induced ROS production in *GhCERK1*-, *GhLYK5*-, and *GhLYK4/5*-silenced cotton plants. Three weeks after VIGS, the leaf discs from the second true leaves were treated with 100 μg/mL of chitin and ROS production was detected at the indicated time-points. The data are shown as the mean ± SE ($n \geq 8$).

(D) Chitin-induced *GhWRKY30* and *GhMPK3* expression in *GhCERK1*, *GhLYK5*, and *GhLYK4/5* silenced cotton plants. Three weeks after VIGS, the true leaves were treated with 100 μg/mL of chitin and collected at 0 and 30 min upon treatment for RT-qPCR. *GhUBQ1* was used as an internal control. The data are shown as mean ± SE from three independent repeats. Asterisks indicate a significant difference using a two-tailed Student's *t* test (*P < 0.05; **P < 0.01).

(E) GhLYK5 complements *atlyk4/5* double mutant on chitin-induced MAPK activation. *GhLYK5-HA* was expressed in wild-type (WT) and *atlyk4/5* mutant protoplasts, respectively. Immunoblot was performed for MAPK activation with an α-pERK1/2 antibody (top), and GhLYK5-HA were detected with an α-HA antibody (middle). Protein loading is shown by Ponceau S for RBC (bottom).

(F) The chitin binding activity of GhCERK1 and GhLYK5 in cotton protoplasts. *GhCERK1-HA*, *GhLYK5-HA*, *GhWAK7A-HA*, or vector control (Ctrl) were expressed in cotton protoplasts. The proteins were immunoprecipitated (IP) with chitin magnetic beads and immunoblotted (IB) with an α-HA antibody (top for IP; middle for input). Protein loading is indicated by Ponceau S staining for RBC (bottom).

(G) and **(H)** Chitin-induced GhCERK1 **(G)** and GhLYK5 **(H)** phosphorylation in cotton protoplasts. Protoplasts expressing *GhCERK1-FLAG* or *GhLYK5-FLAG* were treated with 100 μg/mL of chitin for 0, 15, and 30 min. Total proteins were separated in an 8% SDS-PAGE gel supplemented with 50 μM of Phos-tag (NARD Institute).

(I) GhLYK5 associates with GhCERK1 upon chitin elicitation in cotton protoplasts. *GhLYK5-HA* and *GhCERK1-FLAG* were co-expressed in protoplasts, followed by 100 μg/mL of chitin treatment for 10 min. The association was detected by co-IP with α-FLAG agarose (IP: α-FLAG) and immunoblotting with α-HA (IB: α-HA) or α-FLAG (IB: α-FLAG) antibody (top two panels). The protein inputs are shown with immunoblots before immunoprecipitation (bottom two panels).

The above experiments were repeated at least three times with similar results.

with control plants, the chitin-induced expression of *GhWRKY30* and *GhMPK3* was significantly compromised in *GhCERK1*- or *GhLYK4/5*-silenced plants (Figure 6D). Expression of *GhLYK5* in *atlyk4/5* mutant protoplasts restored chitin-induced MAPK activation (Figure 6E), implying a conserved function of GhLYK5 and AtLYK4/5 mediating the chitin-induced MAPK activation.

Chitin Is Perceived by the GhCERK1 and GhLYK5 Complex in Cotton

Arabidopsis AtLYK5-AtCERK1 is a sensory complex for chitin perception (Cao et al., 2014). We examined whether GhCERK1 and GhLYK5 function similarly in chitin perception and signaling in cotton. *GhCERK1* (*GhCERK1bD*), *GhLYK5* (*GhLYK5D*), or *GhWAK7A* with a hemagglutinin (HA)-tag (*GhCERK1-HA*, *GhLYK5-HA*, or *GhWAK7A-HA*) was expressed in cotton protoplasts and chitin magnetic beads were used to pull down the chitin binding proteins from total proteins isolated from protoplasts. Chitin pulled down GhLYK5 and GhCERK1, rather than GhWAK7A (Figure 6F), suggesting that GhCERK1 and GhLYK5 bind to chitin in cotton. Although GhWAK7A is involved in chitin signaling, it may not bind to chitin directly. Chitin pulled down more GhLYK5 than GhCERK1 (Figure 6F, top), suggesting that GhLYK5 might have a higher affinity to chitin than GhCERK1, as was observed in Arabidopsis (Cao et al., 2014).

Perception of chitin induces the association of AtCERK1 and AtLYK5, and the phosphorylation of AtCERK1 and AtLYK5 in Arabidopsis (Cao et al., 2014; Erwig et al., 2017). Using a Phos-tag gel, we could detect a clear mobility shift of GhCERK1 and GhLYK5 after chitin treatment, indicating chitin-induced phosphorylation of GhCERK1 and GhLYK5 (Figures 6G and 6H). A co-immunoprecipitation (co-IP) assay using cotton protoplasts expressing *GhLYK5-HA* and *GhCERK1-FLAG* revealed that GhLYK5 associated with GhCERK1 upon chitin elicitation (Figure 6I). The chitin-induced GhCERK1 and GhLYK5 phosphorylation were evidenced as mobility shifts in a regular SDS-PAGE analysis (Figure 6I, bottom two panels).

GhWAK7A Complexes with GhCERK1 and GhLYK5

Given that GhWAK7A is involved in chitin-induced early responses and the important roles of GhCERK1 and GhLYK5 in cotton chitin signaling, we tested the potential relationship of GhWAK7A with GhCERK1 and GhLYK5. A co-IP assay in cotton protoplasts co-expressing *GhCERK1-FLAG* with *GhWAK7A-HA* indicated that GhWAK7A-HA coimmunoprecipitated with GhCERK1-FLAG before and after chitin elicitation (Figure 7A). The association of GhWAK7A-HA and GhLYK5-FLAG independent of chitin treatment was observed in a similar assay (Figure 7B) and confirmed using reciprocally switched epitope tags in co-IP assays with GhWAK5A and GhRLP2, a cotton LRR-RLP, as specificity controls (Supplemental Figure 17B). A split-luciferase assay, in which *GhWAK7A* and *GhLYK5* were fused to the N-terminal and C-terminal half of the luciferase gene respectively, further demonstrated the association of GhWAK7A and GhLYK5 in vivo (Figure 7C).

Furthermore, fluorescence lifetime imaging (FLIM)-Förster resonance energy transfer (FRET) measurements revealed that GhLYK5-GFP proteins are in close proximity to GhWAK7A-mCherry, but not to AtBIR2-mCherry, when co-expressed in Arabidopsis protoplasts (Figures 7D and 7E). The FRET efficiency, calculated based on the GFP fluorescence lifetime of GhLYK5-GFP and GhWAK7A-mCherry (8.85% $\pm$ 2.30%), is similar to that of AtBAK1-GFP and AtBIR2-mCherry (9.68 $\pm$ 1.68%; Figures 7D and 7E).

To test whether GhWAK7A directly interacts with GhCERK1 or GhLYK5, we performed an in vitro pull-down assay. The glutathione s-transferase (GST)-fused cytosolic domain of GhLYK5 (GST-GhLYK5^{CD}), immobilized on glutathione-sepharose beads as the bait, specifically pulled down the GhWAK7A cytosolic domain fused to maltose binding protein (MBP) with an HA epitope at the C terminus (MBP-GhWAK7A^{CD}-HA; Figure 7F). Similarly, GST-GhCERK1^{CD} could pull down MBP-GhWAK7A^{CD}-HA proteins (Figure 7G), suggesting a direct interaction of the cytosolic domain of GhWAK7A with the cytosolic domains of GhLYK5 and GhCERK1. These findings imply that although GhWAK7A does not directly bind to chitin, it may modulate the cotton chitin perception complex of GhCERK1 and GhLYK5.

Interestingly, GST-GhCERK1^{CD} could not pull down MBP-GhLYK5^{CD}, supporting the specificity of an in vitro pull-down assay (Figure 7G). The data also indicate that the cytosolic domain of GhCERK1 and GhLYK5 cannot interact with each other directly in the absence of chitin treatment. This is in line with the notion that chitin binds and induces the complex formation of AtCERK1 and AtLYK5 via their extracellular domains in Arabidopsis (Cao et al., 2014; Xue et al., 2019).

GhWAK7A Modulates Chitin-Induced GhCERK1 and GhLYK5 Association and Phosphorylates GhLYK5

We further investigated the potential role of GhWAK7A in complexing with GhCERK1 and GhLYK5. When co-expressed with *GhWAK7A* in cotton protoplasts, the chitin-induced association of GhCERK1 with GhLYK5 was further enhanced (Figure 8A), suggesting that GhWAK7A likely promotes chitin-induced GhCERK1-GhLYK5 complex formation. Because GhWAK7A is a functional kinase (see below), we generated the GhWAK7A kinase-inactive mutant (GhWAK7A^{K451M}) by mutating the Lys residue at position 451 (K^{451}), the predicted ATP binding site to Met (M).

Using this mutant, we performed a co-IP assay to examine the potential role of the GhWAK7A kinase activity in the chitin-induced formation of the GhCERK1-GhLYK5 complex. The co-expression of GhWAK7A^{K451M} dampened the chitin-induced association of GhCERK1-GhLYK5 (Figure 8B). Thus, GhWAK7A modulates chitin sensory complex GhLYK5-GhCERK1 in a kinase-dependent manner. We did not observe any notable effects of GhWAK7A or GhWAK7A^{K451M} on the chitin-induced mobility shift of GhCERK1 or GhLYK5 (Figures 8A and 8B).

We further examined the potential autophosphorylation and transphosphorylation among GhWAK7A, GhCERK1, and GhLYK5. Similar to their counterparts in Arabidopsis (Tanaka et al., 2013; Cao et al., 2014), GST-GhLYK5^{CD} had no detectable kinase activity, and GST-GhCERK1^{CD} had moderate kinase activity in an in vitro kinase assay (Figures 8C and 8D). In contrast, MBP-GhWAK7A^{CD} exhibited strong autophosphorylation activity, whereas MBP-GhWAK7A$^{K451M\text{-}CD}$ showed undetectable phosphorylation activity (Figure 8C). Significantly, MBP-GhWAK7A^{CD} phosphorylated GST-GhLYK5^{CD} (Figure 8C). In addition, different from the phosphorylation of AtLYK5 by AtCERK1 in Arabidopsis (Erwig et al., 2017), neither MBP-GhCERK1^{CD} nor GST-GhCERK1^{CD} phosphorylated GST-GhLYK5^{CD} (Figure 8D; Supplemental Figure 17C).

To test the in vivo phosphorylation of GhLYK5 by GhWAK7A, *GhLYK5-FLAG* was co-expressed with vector control, *GhWAK7A-HA*, or *GhWAK7A*^{K541M}*-HA* in cotton protoplasts with or without chitin treatment, and the phosphorylated GhLYK5-FLAG proteins after immunoprecipitation with FLAG-agarose were detected by anti-phosphoSer/Thr antibody. The results

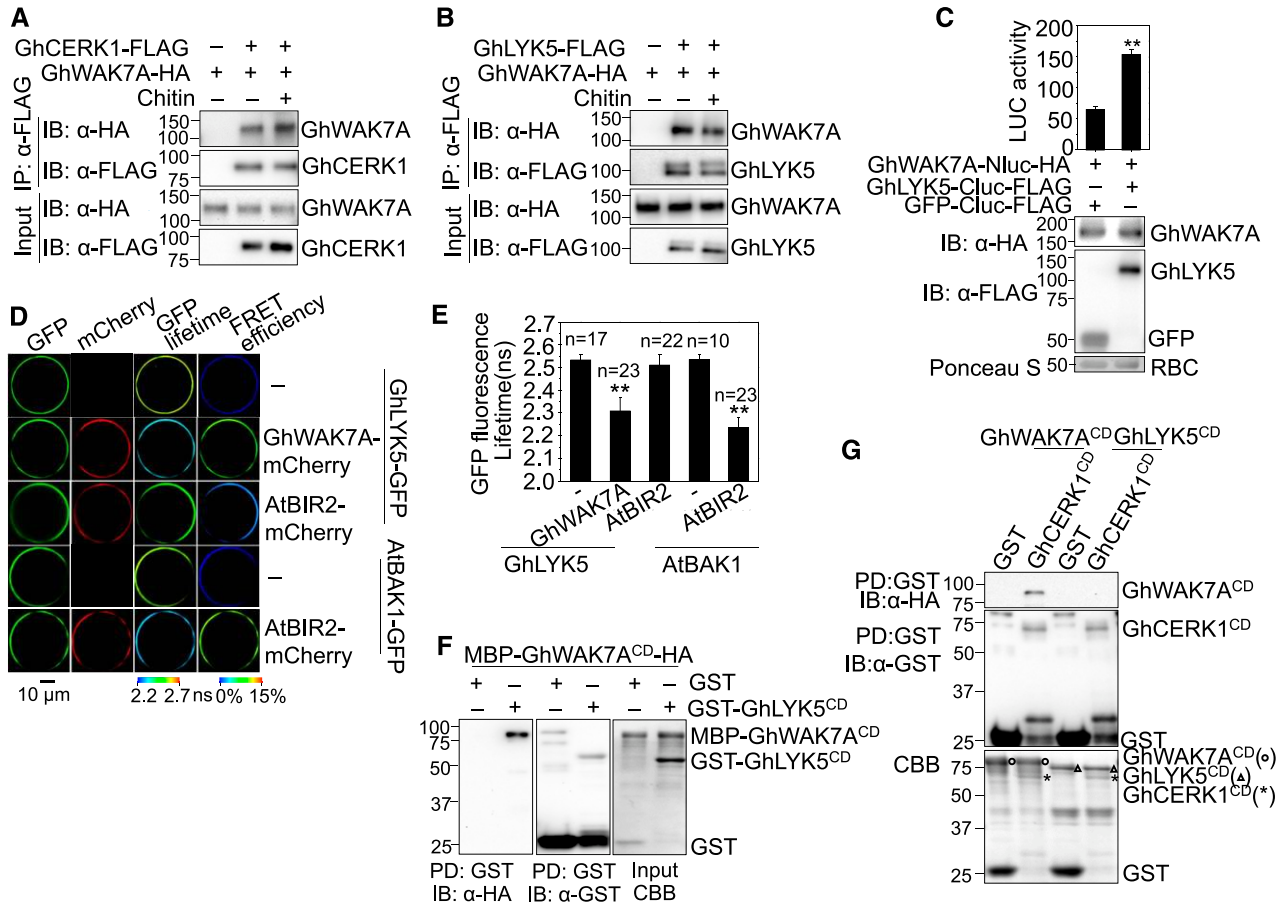

Figure 7. GhWAK7A Interacts with GhCERK1 and GhLYK5.

(A) GhWAK7A associates with GhCERK1 in cotton protoplasts. *GhWAK7-HA* and *GhCERK1-FLAG* were co-expressed in protoplasts, followed by 100 μg/mL of chitin treatment for 10 min. co-IP was performed with α-FLAG agarose (IP: α-FLAG), and the proteins were analyzed by immunoblotting with an α-HA (IB: α-HA) or α-FLAG (IB: α-FLAG) antibody (top two panels). The input controls are shown in the bottom two panels.

(B) GhWAK7A associates with GhLYK5 independent of chitin elicitation in cotton protoplasts. *GhWAK7A-HA* and *GhLYK5-FLAG* were co-expressed in protoplasts followed by 100 μg/mL of chitin treatment for 10 min. The co-IP was performed as in **(A)**.

(C) GhWAK7A associates with GhLYK5 with a split-luciferase assay. *GhLYK5-Cluc-FLAG* or *GFP-Cluc-FLAG* was co-expressed with *GhWAK7A-Nluc-HA* in protoplasts, and luciferase (LUC) activity was detected 12 h after transfection. The data are shown as mean ± SE ($n = 8$). Asterisks indicate a significant difference using a two-tailed Student's *t* test (**P < 0.01). Protein expression is shown on the bottom with immunoblots.

(D) FLIM-FRET analysis of GhLYK5 and GhWAK7A interaction in Arabidopsis protoplasts. The indicated proteins were transiently expressed in Arabidopsis protoplasts for 12 h before imaging analysis. Localization of the GhLYK5-GFP/AtBAK1-GFP and GhWAK7A-mCherry/AtBIR2-mCherry is shown with the first (green) and second column (red), respectively. The lifetime (τ) distribution (third column) and FRET efficiency (fourth column) are presented as pseudo-color images according to the scale. Paired GhLYK5-GFP and AtBIR2-mCherry was used as a negative control, and paired AtBAK1-GFP and AtBIR2-mCherry as a positive control (Halter et al., 2014). Scale bar = 10 μm.

(E) Quantification of lifetimes of GFP signals in **(D)**. The GFP mean fluorescence lifetime (τ) values, ranging from 2.2 to 2.6 ns, were statistically analyzed and are shown as mean ± SD. "n" denotes the number of independent protoplasts. Asterisks indicate statistically significant differences (**P < 0.01), according to a two-tailed Student's *t* test.

(F) GhWAK7A interacts with GhLYK5 in vitro. HA-tagged MBP-GhWAK7A^{CD} (MBP-GhWAK7A^{CD}-HA) was incubated with glutathione beads coupled with GST or GST-GhLYK5^{CD}. The beads were collected and washed for immunoblots with α-HA or α-GST antibodies (left and middle). The protein inputs were determined by Coomassie Brilliant Blue (CBB) staining (right).

(G) GhWAK7A interacts with GhCERK1 in vitro. HA-tagged MBP-fusion proteins (MBP-GhWAK7A^{CD}-HA or MBP-GhLYK5^{CD}-HA) were incubated with glutathione beads coupled with GST or GST-GhCERK1^{CD}. The pull-down assay was performed as in **(F)**.

The above experiments were repeated at least three times with similar results.

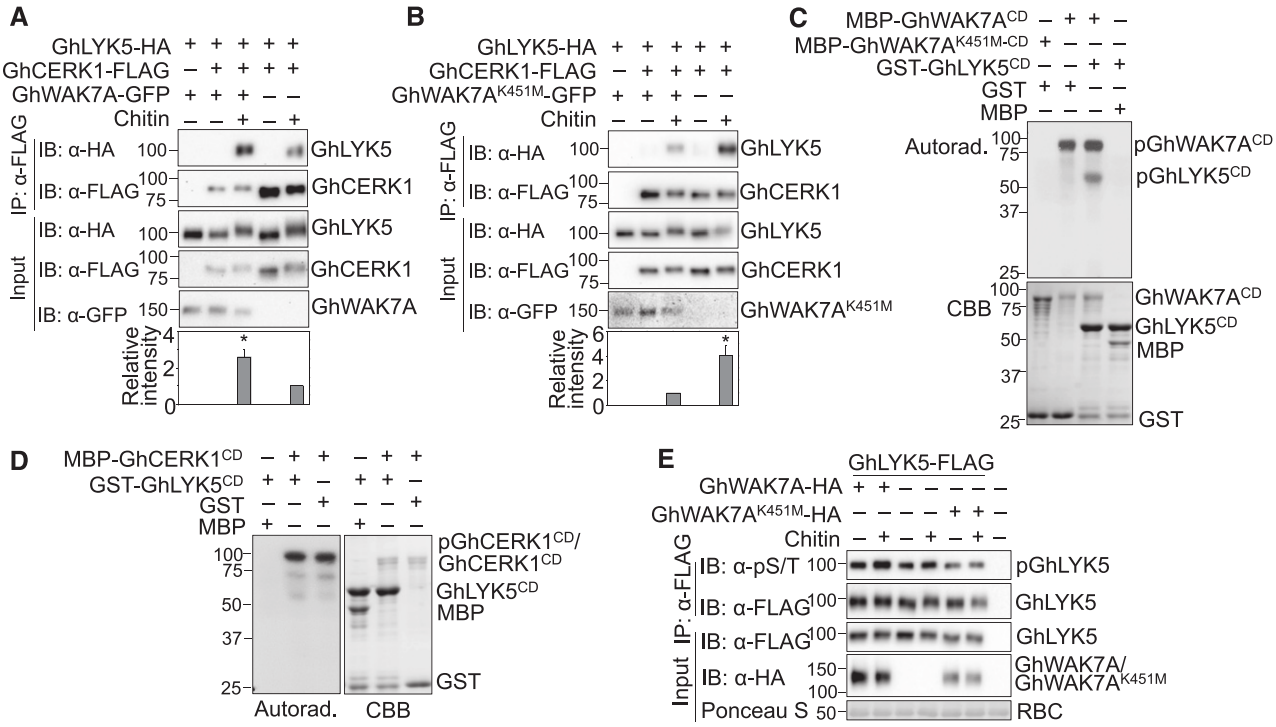

Figure 8. The Phosphorylation of GhLYK5 by GhWAK7A Is Important for Chitin-Triggered Association of GhCERK1 and GhLYK5.

(A) GhWAK7A enhances the chitin-induced GhCERK1-GhLYK5 association. *GhLYK5-HA*, *GhCERK1-FLAG*, and *GhWAK7A-GFP* were co-expressed in protoplasts and treated with 100 μg/mL of chitin for 10 min. Proteins were immunoprecipitated with α-FLAG agarose (IP: α-FLAG) and immunoblotted with α-HA (IB: α-HA) and α-FLAG (IB: α-FLAG) antibodies (top two panels). The protein inputs are shown with immunoblots before immunoprecipitation (middle three panels). The quantification of the densitometry units of immunoprecipitated GhLYK5 normalized to the GhLYK5 inputs are shown on the bottom. The data are shown as mean ± SE from three independent repeats. An asterisk indicates significant differences, according to one-way ANOVA (*$P < 0.05$).

(B) GhWAK7A kinase mutant (GhWAK7A^{K451M}) reduces the chitin-induced GhCERK1-GhLYK5 association. *GhLYK5-HA*, *GhCERK1-FLAG*, and *GhWAK7A^{K451M}-GFP* were co-expressed in protoplasts. GhWAK7A^{K451M} is a kinase-inactive mutant of GhWAK7A with the mutant of Lys **(K)** at position 451 to Met **(M)**. The co-IP assay was performed and analyzed as in **(A)**.

(C) GhWAK7A phosphorylates GhLYK5 in vitro. GST-GhLYK5^{CD} was incubated with MBP-GhWAK7A^{CD} for an in vitro kinase assay using [^{32}P]-γ-ATP. Phosphorylation was detected by autoradiography (top) and the protein loading is shown by Coomassie Brilliant Blue (CBB) staining (bottom).

(D) GhCERK1 cannot phosphorylate GhLYK5 in vitro. GST-GhLYK5^{CD} was incubated with MBP-GhCERK1^{CD} for an in vitro kinase assay using [^{32}P]-γ-ATP. The assay was done as in **(C)**. Phosphorylation was detected by autoradiography (left) and the protein loading is shown by Coomassie Brilliant Blue (CBB) staining (right).

(E) GhWAK7A increases whereas GhWAK7A^{K451M} reduces GhLYK5 phosphorylation in vivo. *GhLYK5-FLAG* was co-expressed with *GhWAK7A-HA* or *GhWAK7A^{K451M}-HA* in protoplasts and treated with or without 100 μg/mL of chitin for 10 min. The GhLYK5 proteins were immunoprecipitated with α-FLAG agaroses (IP, α-FLAG). The immunoprecipitated and input samples were immunoblotted with indicated antibodies. α-pS/T, anti-phosphoSer/Thr antibody. The above experiments were repeated at least three times with similar results.

indicate that GhWAK7A enhanced, whereas GhWAK7A^{K451M} reduced, the phosphorylation of GhLYK5 before and after chitin treatment (Figure 8E). Taken together, the data support the idea that GhWAK7A interacts with and phosphorylates chitin receptor GhLYK5.

DISCUSSION

Cotton fungal vascular diseases, Verticillium and Fusarium wilts, are among the most devastating diseases affecting the yield and quality of cotton worldwide. Chitin, a typical MAMP from the fungal cell wall, triggers defense responses through the activation of PTI. It remains unknown whether there is a conserved chitin perception and signaling system in cotton. In this study, we revealed the chitin sensory complex consisting of GhLYK4/5-GhCERK1 in cotton and established its important role in cotton defense against Verticillium and Fusarium wilt pathogens. Besides, we identified GhWAK7A, a WAK, that is involved in cotton defense against *Vd* and *Fov* by modulating chitin signaling (Figure 9). Without infection, GhWAK7A interacts with GhCERK1 and GhLYK5. Upon fungal pathogen invasions, chitin fragments released from the fungal cell wall are recognized by cotton GhLYK5, which stimulates GhLYK5 association with GhCERK1. Phosphorylation or scaffolding of GhLYK5 by GhWAK7A might promote GhLYK5–GhCERK1 complex formation, which further activates the cytoplasmic signaling events, including ROS production, MAPK activation, and the expression of defense-related genes, to fend off *Vd* and *Fov* infections (Figure 9). Our study reveals that the role of

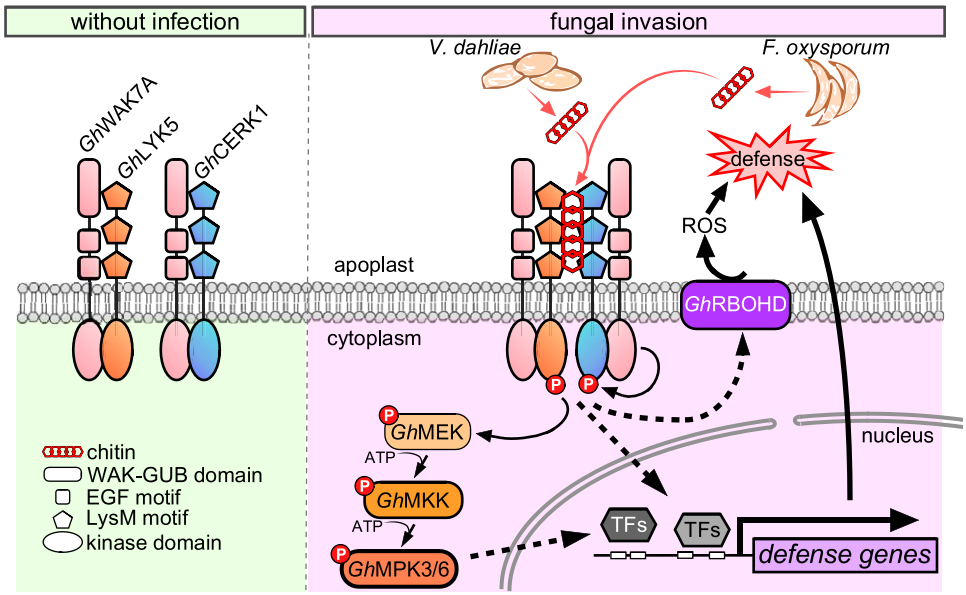

Figure 9. A Proposed Model for GhWAK7A-Mediated Chitin Signaling in Cotton Defense against Fungal Pathogens.

(Left,without infections, GhWAK7A associates with GhLYK5 and GhCERK1, respectively. Right, upon fungal pathogen invasions, chitin fragments released from the fungal cell wall are recognized by cotton GhLYK5, which stimulates GhLYK5 phosphorylation by GhWAK7A and association with GhCERK1. The phosphorylated GhLYK5 might promote and/or scaffold GhLYK5-GhCERK1 complex formation, which further activates the cytoplasmic signaling events, including ROS production, MAPK activation, and the expression of defense-related genes, to fend off *Vd* and *Fov* infections.

GhWAK7A in chitin signaling elucidates the potential mechanism of cotton responses to *Vd* and *Fov*, and provides genetic resources to improve cotton resistance to these two devastating fungal diseases.

Our genome-wide analysis indicates that both *WAK* and *LYK* family genes occurred as a major expansion in terms of gene number after cotton speciation from Arabidopsis, which is consistent with the notion that *G. raimondii* and *G. arboreum* underwent cotton-specific, whole-genome duplication ~16.6 million years ago after the paleohexaploidization event common to all eudicots (Wang et al., 2012). The cotton *LYK* family was divided into five clades corresponding to the five members in Arabidopsis, indicating that the five *LYK* members had already evolved before cotton and Arabidopsis speciation. The high syntenic relationships between A-subgenome *GhLYKs* and *GaLYKs*, and between D-subgenome *GhLYKs* and *GrLYKs*, exemplified that the hybridization of an A-genome ancestor resembling *G. arboreum* with a D-genome ancestor resembling *G. raimondii* gave rise to the speciation of *G. hirsutum* (Paterson et al., 2012).

Different from *LYKs*, *WAKs* may have evolved independently after cotton and Arabidopsis speciation. Most cotton *WAKs* are clustered in a pattern that is consistent across the tetraploid and diploid species, similar to the *WAK* family distribution in Arabidopsis and rice (He et al., 1999; Zhang et al., 2005). Thus, tandem duplication plays a dominant role in the expansion of *WAKs* in different plant species, including both monocots and dicots. The different numbers of *WAK*s among different cotton species and their phylogenetic comparisons suggest that a large portion of *WAKs* in *G. arboreum*, especially those in chromosome 10, were lost during the polyploidization and speciation of *G. hirsutum*. This may contribute to the reduction of the *G. hirsutum* genome size after allopolyploidization (Li et al., 2015). Moreover, gene translocations were evident in several *WAKs* during the speciation of *G. hirsutum*. The conservation of *LYKs* and the divergence of *WAKs* in different plant species may support their biological functions, with LYKs as chitin receptors perceiving conserved fungal MAMPs and WAKs as the signaling components modulating PTI signaling.

LYKs, a type of RLK with extracellular LysM-domains, function in β-1,4-linked N-acetylglucosamine-containing microbial pattern perception, signaling, and plant immunity to fungal pathogens (Tanaka et al., 2013; Kawasaki et al., 2017). Most *GhLYKs* are upregulated upon *Vd* infection in cotton. GhCERK1 and GhLYK5 are required for cotton defense against fungal wilt pathogens. CERK1 is a critical component for chitin signaling in rice and Arabidopsis (Miya et al., 2007; Shimizu et al., 2010). GhCERK1, with 60% protein identity to AtCERK1, was demonstrated here to be essential for chitin-induced defense responses including MAPK activation, ROS production, and defense gene expression against fungal infection. AtLYK4 and AtLYK5 are involved in chitin sensing and share overlapping functions (Wan et al., 2012; Cao et al., 2014), and are required for plant defense against *Vd* and *Fo* '5176'. The simultaneous knockdown of *GhLYK4* and *GhLYK5* (*GhLYK4/5*) exhibited compromised chitin-induced responses in cotton, similar to the *atlyk4/5* double mutant. AtLYK5 exhibited higher chitin binding affinity than AtCERK1, and forms a chitin-induced complex with AtCERK1 (Cao et al., 2014). Similarly, in cotton, GhLYK5 likely binds to chitin with higher affinity than GhCERK1 and associates with GhCERK1 in a chitin-dependent manner. Chitin induces the phosphorylation of GhLYK5 and GhCERK1 in vivo. In Arabidopsis, although the AtLYK5 kinase

domain is inactive, it is required for chitin-induced association with AtCERK1, AtCERK1 phosphorylation, and activation of defense responses including ROS production and MAPK activation (Cao et al., 2014). Chitin-induced AtLYK5 phosphorylation is AtCERK1-dependent, which phosphorylates AtLYK5 in vitro (Erwig et al., 2017). Different from the observation in Arabidopsis that AtCERK1 phosphorylates AtLYK5 in vitro (Erwig et al., 2017), GhCERK1 has a moderate kinase activity, but it cannot phosphorylate GhLYK5. The data suggest that another kinase in the chitin sensory complex, likely GhWAK7A identified in our study, could phosphorylate and/or scaffold GhLYK5; this may promote chitin-induced GhLYK5-GhCERK1 complex formation, thereby activating downstream signaling.

WAKs compose a unique group of RLKs that likely associate with the pectin in the cell wall, and are necessary for both cell expansion during development and mediation of the response to pathogens (Kohorn and Kohorn, 2012). In cotton, eight *GhWAKs* were upregulated within 1 d after infection with *Vd*. Among them, *GhWAK7A* positively regulates cotton defense against fungal pathogens, *Vd* and *Fov*. Similarly, members of rice *OsWAKs* were transcriptionally upregulated by chitin treatment and quantitatively contribute to resistance against rice blast fungus *Magnaporthe oryzae* (Delteil et al., 2016). GhWAK7A is involved in chitin-induced immune responses in cotton but does not bind to chitin directly. Furthermore, GhWAK7A interacts with GhCERK1 and GhLYK5 and phosphorylates GhLYK5 in vivo and in vitro. GhWAK7A promotes chitin-induced GhCERK1-GhLYK5 dimerization depending on the GhWAK7A kinase activity. The data suggest that GhWAK7A contributes to the chitin-induced phosphorylation of GhLYK5. This was further supported by the in vivo phosphorylation study in which GhWAK7A increased whereas the kinase-inactive GhWAK7A^{K451M} reduced phosphorylation of GhLYK5. In light of the observations that the AtLYK5 kinase domain and AtCERK1 phosphorylation are required for the AtLYK5-AtCERK1 complex formation and initiating chitin signaling (Cao et al., 2014; Liu et al., 2018), it is tempting to speculate that the phosphorylation and/or scaffolding of GhLYK5 by GhWAK7A promotes GhLYK5 association with GhCERK1 upon chitin perception, which subsequently activates downstream signaling.

WAKs have been reported to be associated with the perception of OGs and cell wall components in Arabidopsis (Kohorn and Kohorn, 2012). We tested whether GhWAK7A is involved in the responses triggered by OGs, the potential ligand of AtWAK1 (Brutus et al., 2010). Silencing *GhWAK7A* did not affect OG-triggered MAPK activation, ROS production, or gene expression, suggesting that GhWAK7A might not be involved in OG responses. Besides, GhWAK7A did not contribute to the MAPK activation triggered by FovCWE, an unknown elicitor isolated from *Fo* cell wall. Alternatively, GhWAK7A might perceive an unknown ligand from *Vd* and *Fov* to activate defense signaling. Nevertheless, our study sheds light on the underlying mechanisms of WAKs in plant disease resistance against various fungal pathogens.

METHODS

Cotton WAK and LYK Family Gene Identification

The identification and phylogenetic analyses of cotton (*Gosspuim* spp) WAK and LYK families were conducted among three cotton species—allotetraploid *Gossypium hirsutum*, diploid *Gossypium arboreum*, and *Gossypium raimondii*. The five Arabidopsis (*Arabidopsis thaliana*) WAK (WAK1-AT1G21250, WAK2-AT1G21270, WAK3-AT1G21240, WAK4-AT1G21210, and WAK5-AT1G21230) or LYK (CERK1-AT3G21630, LYK2-AT3G01840, LYK3-AT1G51940, LYK4-AT2G23770, and LYK5-AT2G33580) protein sequences were used as the queries for a BLASTp search against three cotton protein databases: *G. hirsutum* (AD_1; NAU assembly), *G. arboreum* (A_2; CRI assembly), and *G. raimondii* (D_5; JGI assembly) employing a threshold E-value < 1e-50 from the CottonFGD (https://cottonfgd.org/).

The candidates from all five queries for WAK or LYK were combined to form the primary list. From this list, protein sequences found to not belong to either the WAK or the LYK family, based on the annotation or the reduplicative proteins, were deleted. Next, we manually checked each protein motifs using the programs SMART (http://smart.embl-heidelberg.de/) and Interpro (https://www.ebi.ac.uk/interpro/) prediction. Proteins with a signal peptide, a transmembrane domain, a kinase domain, and extracellular WAK_GUB, EGF, and EGF_Ca^{2+} domains for WAK, or LysM motif, or an annotated similarity to the PDB:4EBZ structure for LYK, were regarded as cotton WAK or LYK family proteins. Using this refined set of putative WAK and LYK full-length protein or kinase domain sequences, phylogenetic trees were built by the neighbor-joining method with 1,000 bootstrap replicates using the program MEGA X (Kumar et al., 2018). The exon–intron structures were analyzed by aligning the genomic DNA sequences with their corresponding coding sequences using the Gene Structure Display Server (v2.0; http://gsds.cbi.pku.edu.cn/).

Plant Materials and Growth Conditions

G. hirsutum 'CA 4002' (PI 665226) was grown in 3.5-inch square pots containing PRO-LINE C/25 soil (Jolly Gardener) at 23°C, 30% humidity, and 100 $\mu E\ m^{-2}\ s^{-1}$ light (bulb type; Philips F40T12/DX) with a 12-h light/12-h dark photoperiod. Two-week-old cotton plants were used for Agrobacterium (*Agrobacterium tumefaciens*)-mediated VIGS assays and protoplast isolation. Three weeks after VIGS, plants were inoculated with *Verticillium dahliae* (*Vd*) 'King' isolate or *Fusarium oxysporum* f. sp *vasinfectum* (*Fov*) CA10.

Arabidopsis mutants *atcerk1* (GABI-KAT 096F09), *atlyk4* (CS850683), *atlyk5-2* (SALK_131911C), and *atlyk4/atlyk5-2* (*atlyk4/5*) were obtained from Gary Stacey (Cao et al., 2014). The mutants and wild-type plants were grown in soil (Metro Mix 366) in a growth room at 23°C, 45% humidity, and 75 $\mu E\ m^{-2}\ s^{-1}$ light with a 12-h light/12-h dark photoperiod. Three-week-old plants were inoculated with *Vd* 'King' isolate or *Fusarium oxysporum* (*Fo*) '5176'. Four-week-old plants were used for chitin-induced MAPK activation and ROS production assays.

Fungal Preparation and Inoculation

Vd 'King' isolate (Terry Wheeler, Texas A&M), *Fov* CA10 (Mike Davis, University of California at Davis), and *Fo* '5176' (Lijun Ma, University of Massachusetts at Amherst) were grown on potato dextrose agar plates (Difco) for 4 d at room temperature (23°C) for *Vd*, or 28°C for *Fov* and *Fo* '5176'. The hyphae of *Vd* were inoculated in Czapek medium ($NaNO_3$, 0.2% [w/v]; $MgSO_4$, 0.05% [w/v]; KH_2PO_4, 0.1% [w/v]; $FeSO_4$, 0.001% [w/v]; KCl, 0.05% [w/v]; Suc, 3% [w/v]; pH 7.3 $\pm$ 0.2) and incubated in a shaker (120 rpm) at 23°C for 5 d. The hyphae of *Fov* and *Fo* '5176' were inoculated in potato dextrose broth (Difco) and incubated in a shaker (120 rpm) at 28°C for 5 d. The spores were collected from the medium by filtering through Miracloth (Millipore). After centrifugation at 4,000 rpm for 15 min, the spores were resuspended with sterile water and adjusted to the final concentration. The inoculum used for *Vd* inoculation was 1×10^6 spores/mL and 1×10^7 spores/mL for *Fov* and *Fo* '5176'.

The root-dipping method was used for both cotton and Arabidopsis inoculation as previously reported by Gao et al. (2013a, 2013b). Briefly,

three weeks after VIGS, cotton seedlings were removed from soil and the roots were dip-infected with *Vd* or *Fov* spore suspension for 3 min. The seedlings were then replanted in fresh soil. For Arabidopsis, 3-week-old seedlings were gently uprooted from soil and the roots were briefly washed with water to remove big chunks of soil. After the removal of excess water with paper towels, the roots were immersed in the *Vd* or *Fo* '5176' spore suspension for 3 min and then planted in pots with pre-wet soil. The cotton and Arabidopsis seedlings inculated with *Vd* were put back to the same growth room as they were before the infection, respectively. After inoculation with *Fov* or *Fo* '5176', plants were transferred into a growth chamber at 28°C, 50% humidity, and 100 $\mu E\, m^{-2}\, s^{-1}$ light with a 12-h light/12-h dark photoperiod.

Hydroponic Growth of Cotton and Salt Treatment

The hydroponic growth and salt treatment of cotton were performed as previously described by Mu et al. (2019) with minor modifications. *G. hirsutum* 'CA 4002' (PI 665226) seeds were surface-sterilized by gently shaking in 9% (v/v) H_2O_2 for 20 min, rinsed five times with sterile water, and covered with two-layer, pre-wet paper towels in a box at 28°C under 80 $\mu E\, m^{-2}\, s^{-1}$ light. Three d post germination, the uniformly germinated seedlings were transplanted and suspended into containers with Hoagland solution (Micronutrients: 20 μM of H_3BO_3, 1 μM of $ZnSO_4 \cdot 7H_2O$, 0.1 μM of $CuSO_4 \cdot 5H_2O$, 1 μM of $MnSO_4 \cdot H_2O$, and 5 nM of $(NH_4)_6Mo_7O_{24}$; Macronutrients: 0.1 mM of EDTA·FeNa, 2.5 mM of $Ca(NO_3)_2 \cdot 4H_2O$, 0.5 mM of $NH_4H_2PO_4$, 1 mM of $MgSO_4 \cdot 7H_2O$, and 2.5 mM of KNO_3). The Hoagland solution was agitated to ensure the proper root aeration and replaced freshly once a week. Seedlings were grown at 23°C, 60% humidity, and 80 $\mu E\, m^{-2}\, s^{-1}$ light with a 14-h light/10-h dark photoperiod. Three d after transplantation, cotton cotyledons were infiltrated with Agrobacterium for VIGS. Three weeks after VIGS, NaCl were added into Hoagland solution for a final concentration of 200 mM as salt treatment.

Disease Severity Quantification and Observation

The disease severity of cotton plants was evaluated via DI based on the foliar symptom and stem vascular discoloration. The DI was calculated as previously described by Xu et al. (2012) with minor modifications. The cotyledons of cotton seedlings after VIGS were not considered for disease symptoms as the hand-infiltration of Agrobacterium may introduce damage. For VIGS cotton plants, the severity of the disease symptoms on each cotton seedling was scored using a 0-to-4 rating scale, where 0 = no visible chlorosis or wilting symptoms; 1 = one true leaf showed chlorosis or wilting symptoms; 2 = two true leaves wilted or dropped off; 3 = more than two true leaves wilted or dropped off; and 4 = the whole plant wilted or all leaves dropped off. The DI was calculated according to the following formula: $DI = (1n_1 + 2n_2 + 3n_3 + 4n_4) \times 100/4N_t$, where n_1 to n_4 is the number of plants in the indicated scale, and N_t is the total number of plants tested. For stem discoloration observation, the transaction slices of fresh stems ~1.5 cm above the soil-line were collected and examined under an optical microscope (model no. SZX10; Olympus).

The disease scales for Arabidopsis disease investigation are as follows: 0 = healthy plants; upon fungal infection, 1 = 0% to 25% of the leaves show chlorosis around the vein of leaves; 2 = 25% to 50% of the leaves show chlorosis or wilting; 3 = 50% to 75% of the leaves show chlorosis or wilting; and 4 = 75% to 100% of the leaves show chlorosis or wilting. The DI was calculated using the formula described above.

Elicitor Preparations

Chitin fragments were suspended in sterile water after sonication of chitin from shrimp shells (Sigma-Aldrich) and used at a final concentration of 100 μg/mL. OGs were obtained from pure polygalacturonic acid (Alfa Aesar) by enzymatic digestion with purified polygalacturonase from *Aspergillus niger* (AnPGII), dialysis, and ethanol precipitation, as previously described by Pontiggia et al. (2015). High-performance anion-exchange chromatography with pulsed amperometric detection profiles and electrospray ionization mass spectrometry spectra of OGs were obtained in an electrospray ionization LTQ-Orbitrap mass spectrometer (Thermo Fisher Scientific) in a positive ion mode as previously described by Benedetti et al. (2017). OGs were dissolved in sterile water at a final concentration of 100 μg/mL. FovCWE from *Fov* 'CA10' was prepared according to Davies et al. (2006), and dissolved in sterile water at a final concentration of 1 mg/mL.

Plasmid Construction

The conserved regions of the A- and D-subgenome copies and homoeologs of *GhCERK1* (439 bp), *GhLYK2* (472 bp), *GhLYK3* (539 bp), *GhLYK4* (281bp), and *GhLYK5* (636 bp), and the fragments *of GhWAK5A* (446 bp) and *GhWAK7A* (445 bp) were amplified from cotton (*G. hirsutum*) cDNA, and inserted into the *pYL156* (*pTRV-RNA2*) vector with restriction-enzyme *Eco*RI and *Kpn*I digestion for VIGS assays. The VIGS-*GhCLA1*, *GhMPK6*, and *GhMPK3* constructs were previously reported by Gao et al. (2011) and Li et al. (2017a). To generate the VIGS-*GhLYK4/GhLYK5* (*GhLYK4/5*) construct, fragments of *GhLYK4* (336 bp) and *GhLYK5* (279 bp) were PCR-amplified from cotton cDNA, digested with *Eco*RI and *Nco*I for the *GhLYK5* fragment, and *Nco*I and *Kpn*I for the *GhLYK4* fragment, and ligated simultaneously with the *pYL156* (*pTRV–RNA2*) vector-digested with *Eco*RI and *Kpn*I. The full-length *GhCERK1*, *GhLYK5*, *GhWAK7A*, *GhWAK5A*, and *GhRLP2* genes were amplified from cotton cDNA with primers containing *Bam*HI, *Spe*I, or *Nco*I in the forward primers and *Eco*RV, *Stu*I, or *Sma*I in the reverse primers, and introduced into the plant gene expression vector *pHBT* with an HA, FLAG, or GFP epitope-tag at the C terminus. *pHBT-p35S::GFP-Cluc-FLAG* was generated by PCR-amplifying *GFP* from *pHBT-p35S::GFP* and sub-cloned into *pHBT-p35S::Cluc-FLAG* by *Bam*HI and *Spe*I digestion. *Cluc* (1,291 to 1,746 bp) was amplified from *pHBT-pFRK1::LUC*. *pHBT-p35S::GhLYK5-CLuc-FLAG* was generated by PCR-amplifying *GhLYK5* from *pHBT-p35S::GhLYK5-HA* and sub-cloned into *pHBT-p35S::Cluc-FLAG* using a one-step cloning kit by *Bam*HI and *Spe*I digestion. *Nluc* (457 to 1,746 bp) was amplified from *pHBT-pFRK1::LUC*. *pHBT-p35S::GhWAK7-Nluc-HA* was generated by PCR-amplifying *GhWAK7A* from *pHBT-p35S::GhWAK7A-HA* and sub-cloned into *pHBT-p35S::NLuc-FLAG* using a one-step cloning kit by *Bam*HI and *Spe*I digestion.

For FLIM-FRET constructs, genes of interest tagged by the fluorescence protein GFP or mCherry were developed according to Bajar et al.. (2016). Briefly, *AtBAK1* fragment was released from *pHBT-p35S::AtBAK1-FLAG* by *Bam*HI and *Stu*I digestion and ligated into the *pHBT* vector with a GFP epitope-tag at C terminus, resulting in *pHBT-p35S::AtBAK1-GFP*. The GFP-Nos terminator fragment was released from *pHBT-p35S::AtBAK1-GFP* by *Stu*I and *Eco*RI digestion, and ligated into *pHBT-p35S::GhLYK5-HA* with the same enzyme digestion, resulting in *pHBT-p35S::GhLYK5-GFP*. Similarly, the *AtBIR2* fragments were released from *pHBT-p35S::AtBIR2-FLAG* by *Bam*HI and *Stu*I digestion and ligated into the *pHBT* vector with a mCherry epitope-tag at C terminus, resulting in *pHBT-p35S::AtBIR2-mCherry*. The mCherry-Nos terminator fragment was released from *pHBT-p35S::AtBIR2-mCherry* by *Stu*I and *Eco*RI digestion, and ligated into *pHBT-p35S::GhWAK7A-HA* with the same enzyme digestion, resulting in *pHBT-p35S::GhWAK7A-mCherry*. The point mutation of $GhWAK7A^{K451M}$ was generated by a site-directed mutagenesis kit using the wild-type *GhWAK7A* plasmid as the template. For *Escherichia coli* fusion protein constructs, the cytosolic domains of *GhCERK1* (703 to 1,860 bp), *GhLYK5* (922 to 2,010 bp), *GhWAK7A* (1,120 to 2,256 bp), and $GhWAK7A^{K451M}$ (1,120 to 2,256 bp) were amplified with primers containing *Bam*HI or *Bgl*II in the forward primers and *Eco*RV or *Stu*I in the reverse

primers, and introduced into a modified GST fusion protein expression vector *pGEX4T-1* (Pharmacia) or a modified *pMAL-c2* vector (New England BioLabs) with *Bam*HI and *Stu*I digestion. The recombinant fusion protein expression vectors were introduced into *E. coli* strain BL21 (DE3). Expression of fusion proteins and affinity purification were performed following the standard protocol provided by the manufacturers. The primers for cloning and point mutations are given in Supplemental Table 15, and all the clones were confirmed by Sanger-sequencing.

RNA Isolation and RT-qPCR Analysis

To measure *Vd*-induced gene expression, 2-week-old cotton seedlings were inoculated with *Vd* 'King' isolate spores by the root-dipping method (Gao et al., 2013a). Root samples were harvested at the indicated time-points. To evaluate gene silencing efficiency, three weeks after VIGS infiltration, the second true leaves or roots were collected. For chitin- or OGs-induced gene expression in VIGS-silenced cotton, three weeks after Agrobacterium infiltration, 10 leaf discs (7.5-mm diameter) from the second true leaves of three individual plants for each sample were soaked in 100 μg/mL of chitin or 100 μg/mL of OGs solution and harvested at 0 and 30 min. Cotton total RNAs were extracted from roots and leaves using a Spectrum Plant Total RNA Kit (Sigma-Aldrich) according to the manufacturer's protocol and quantified using a NanoDrop spectrophotometer (Thermo Fisher Scientific). RNAs were then reverse-transcribed to synthesize the first-strand cDNAs with M-MuLV Reverse Transcriptase and oligo (dT) primers after RNase-free DNase I (New England Biolabs) treatment. RT-qPCR analysis was performed with the primers listed in Supplemental Table 15, using iTaq SYBR green Supermix (Bio-Rad) and a CFX384 Real-Time PCR System (Bio-Rad) following a standard protocol. The expression of each gene was normalized to the expression of *GhUBQ1*.

Agrobacterium tumefaciens-Mediated VIGS

Plasmids containing binary TRV vectors *pTRV-RNA1* and *pTRV-RNA2* derivatives, *pYL156-GhCERK1*, *pYL156-GhLYK2*, *pYL156-GhLYK3*, *pYL156-GhLYK4*, *pYL56-GhLYK5*, *pYL56-GhWAK7A*, *pYL56-GhLYK5A*, *pYL156-GhLYK4/5*, *pYL156-GhCLA1*, and *pYL156-GFP* (Ctrl) were introduced into Agrobacterium strain GV3101 by electroporation. The Agrobacterium cultures carrying the above pTRV-RNA1 and individual pTRV-RNA2 derivative were mixed after resuspension with infiltration buffer (10 mM of $MgCl_2$, 10 mM of MES, and 200 μM of acetosyringone) and infiltrated into cotyledons of 2-week-old cotton plants (Gao et al., 2011). The silencing of *GhCLA1*, which leads to a plant albino phenotype, was included as a visual marker for VIGS efficiency. Three weeks after VIGS, the silenced plants were subjected to elicitor treatments or inoculation with the indicated fungal pathogens.

MAPK Assay

The leaf discs (7.5-mm diameter) from the second true leaves of VIGS cotton or 4-week-old Arabidopsis plants were soaked in distilled water overnight, then treated with 100 μg/mL of chitin, 100 μg/mL of OGs, or 1 mg/mL of FovCWE at the time-points indicated in each figure. Each sample contained two leaf discs from different plants and was grounded in 100 μL of SDS buffer (62.5 mM of Tris-HCl at pH 6.8, 1% [w/v] SDS, 0.025% [w/v] bromophenol blue, 10% [v/v] glycerol, 4% [v/v] β-mercaptoethanol,1 × protease inhibitor, 2 μM of NaF, and 2 μM of Na_3VO_4) before being boiled at 95°C for 10 min. This boiled homogenate was centrifuged at 14,000*g* for 10 min at 4°C, and the supernatant was collected and loaded onto 10% SDS-PAGE gels before transfer to a polyvinylidene difluoride membrane, which was subsequently blotted using an anti-phosphorylated extracellular-regulated protein kinase 1/2 antibody (cat. no. 9101, dilution 1:2,000 [v/v]; Cell Signaling) for the detection of pMPK3/6, an α-MPK6 antibody (cat. no. A7104, dilution 1:10,000 [v/v]; Sigma-Aldrich) for the detection of MPK6 proteins, or an α-MPK3 antibody (cat. no. M8318, dilution 1:4,000 [v/v]; Sigma-Aldrich) for MPK3 proteins.

ROS Assay

ROS burst was determined by a luminol-based assay. The third and fourth pairs of true leaves from 4-week-old Arabidopsis or the second true leaves from cotton were excised into leaf discs (5-mm diameter). These discs were subjected to overnight incubation in a 96-well plate with 100 μL of distilled water to allow the immediate wounding effects to subside. Next, the water in each well was replaced by 100 μL of reaction solution containing 50 μM of luminol and 10 μg/mL of horseradish peroxidase (Sigma-Aldrich) supplemented with 100 μg/mL of chitin or 100 μg/mL of OGs. The measurement was conducted immediately after adding the solution with a luminometer (model no. Victor X3; Perkin-Elmer), with a 1-min interval reading time for a period of 20 min for cotton or 30 min for Arabidopsis. The values for ROS production from each line were indicated as means of relative light units.

Chitin Binding Assays

The in vivo chitin binding assay was performed as described in Petutschnig et al. (2010) and Gu et al. (2017) with modifications. The *GhCERK1*, *GhLYK5*, and *GhWAK7A* in *pHBT* vector with an HA tag and vector control were expressed in 500 μL of cotton protoplasts (2×10^5 cells/mL) for 12 h. The cells were lysed by extraction buffer (100 mM of NaCl, 1 mM of EDTA, 20 mM of Tris-HCl at pH 7.5, 2 mM of NaF, 2 mM of Na_3VO_4, 1 mM of DTT, 0.5% [v/v] Triton X-100, 10% [v/v] glycerol, and 1 × protease inhibitor). The cell lysis was centrifuged at 12,500*g* at 4°C for 15 min, the supernatant mixture was incubated with chitin magnetic beads (New England Biolabs) at 4°C for 3 h. The incubated beads were rinsed five times with washing buffer (100 mM of NaCl, 1 mM of EDTA, 20 mM of Tris-HCl, and 0.1% [v/v] Triton X-100). After 95°C boiling for 10 min in SDS loading buffer (62.5 mM of Tris-HCl pH 6.8, 1% [w/v] SDS, 0.025% [w/v] bromophenol blue, and 10% [v/v] glycerol), the immunoprecipitated and input proteins were analyzed by immunoblotting with an α-HA antibody (cat. no. 12013819001, dilution 1:2,000 [v/v]; Roche).

Co-IP Assay

Cotton protoplasts were isolated from cotyledons of 2-week-old seedlings (Gao et al., 2011), transfected with indicated constructs (1 mL of protoplasts with 2×10^5 cells), incubated for 12 h and followed by treatment with 100 μg/mL of chitin for 10 min. Samples were collected by centrifugation and lysed with co-IP buffer (20 mM of Tris-HCl at pH 7.5, 100 mM of NaCl, 1 mM of EDTA, 10% [v/v] glycerol, 0.5% [v/v] Triton X-100, 1 × protease inhibitor, 1 mM of DTT, 2 mM of Na_3VO_4, and 2 mM of NaF). Protein extracts were incubated with FLAG-agarose beads (cat. no. 2220; Sigma-Aldrich) for 2 h at 4°C. The beads were collected and washed three times with washing buffer (20 mM of Tris-HCl at pH 7.5, 100 mM of NaCl, 1 mM of EDTA, and 0.1% [v/v] Triton X-100), and once with 50 mM of Tris-HCl at pH 7.5. The immunoprecipitated and input proteins were analyzed by immunoblotting with an α-HA (cat. no. 12013819001, dilution 1:2,000 [v/v]; Roche), α-FLAG (cat. no. A8592, dilution 1:2,000 [v/v]; Sigma-Aldrich) or α-GFP (cat. no. 11814460001, dilution 1:2,000 [v/v]; Roche) antibody as indicated.

In Vitro Pull-Down Assay

The GST, GST-GhCERK1^{CD}, and GST-GhLYK5^{CD} proteins were purified with Pierce glutathione agaroses (Thermo Fisher Scientific), and the MBP-GhLYK5^{CD} and MBP-GhWAK7A^{CD} proteins were purified with amylose

resins (New England Biolabs) according to the protocols from the manufacturers. MBP-GhWAK7A^{CD} or MBP-GhLYK5^{CD} (2 μg) was used as prey and pre-incubated with glutathione agaroses in 300 μL of co-IP buffer (20 mM of Tris-HCl at pH 7.5, 100 mM of NaCl, 1 mM of EDTA, 10% [v/v] glycerol, 0.5% [v/v] Triton X-100, 1 × protease inhibitor, 1 mM of DTT, 2 mM of Na_3VO_4, and 2 mM of NaF) for 0.5 h at 4°C. The supernatants after centrifugation were collected and incubated with 5 μL of pre-washed GST, GST-GhCERK1^{CD}, or GST-GhLYK5^{CD} agarose beads for an additional 1 h. The beads were collected and washed three times with washing buffer (20 mM of Tris-HCl at pH 7.5, 100 mM of NaCl, 1 mM of EDTA, and 0.1% [v/v] Triton X-100), and once with 50 mM of Tris-HCl at pH 7.5. The MBP proteins were tagged with an HA epitope at the C terminus and were detected with an α-HA antibody (cat. no. 12013819001, dilution 1:2,000 [v/v]; Roche) by immunoblotting. GST fusion proteins are shown by immunoblotting with an α-GST antibody (cat. no. SC-53909, dilution 1:2,000 [v/v]; Santa Cruz Biotechnology).

Split-Luciferase Assay

GhWAK7A-Nluc-HA was co-expressed with *GhLYK5-Cluc-FLAG* or *GFP-CLuc-FLAG* in 200 μL of cotton protoplasts (2×10^5 cells/mL) for 12 h. The cells were lysed in extraction buffer (100 mM of NaCl, 1 mM of EDTA, 20 mM of Tris-HCl at pH 7.5, 2 mM of NaF, 2 mM of Na_3VO_4, 1 mM of DTT, 0.5% [v/v] Triton X-100, 10% [v/v] glycerol, and 1 × protease inhibitor). The cell lysate was collected after 10 min of centrifugation at 4°C. The luciferase activity of the supernatant was measured with 0.2 mM of luciferin with a luminometer (Perkin Elmer). The protein level was detected with immunoblotting using α-HA (cat. no. 12013819001, dilution 1:2,000 [v/v]; Roche) and α-FLAG (cat. no. A8592, dilution 1:2,000 [v/v]; Sigma-Aldrich) antibodies.

Confocal Microscopy and FLIM-FRET Assays

The FLIM-FRET assay was performed in an Arabidopsis protoplast system. Plasmid DNAs *pHBT-GhLYK5-GFP* was co-transformed with *pHBT-GhWAK7A-mCherry* or *pHBT-AtBIR2-mCherry* into protoplasts and incubated for 12 h. *pHBT-BAK1-GFP* and *pHBT-AtBIR2-mCherry* were included as the positive control. Protoplasts were examined for FLIM performed on a TCS SP8 confocal laser scanning microscope (Leica) equipped with time-correlated single-photon counting electronics (PicoHarp 300; PicoQuant), photon-sensitive detectors (HyD detector), and a pulsed laser (white light laser). The GFP fluorescence was excited at 488 nm, and emissions were detected between 490 and 530 nm. The mCherry fluorescence was excited at 587 nm, and emissions were detected between 590 and 620 nm. The pinhole was set at 1 Airy unit. Images and FLIM/FRET calculation were recorded and performed using the Leica Application Suite X software as described by Bücherl et al. (2010). GFP fluorescence lifetime (τ) is normally an amplitude-weighted mean value using the data from the single (GFP-fused donor protein only) or biexponential fit (GFP-fused donor protein interacting with mCherry-fused acceptor protein). FRET efficiency (*E*) was calculated by comparing the lifetime of the donor in the presence of τDA or absence τD of the acceptor according to the following formula: $E = 1-(\tau_{DA}/\tau_D)$. Mean lifetimes were presented as means ± SD ($n \geq 10$).

In Vitro Kinase Assays

One μg of MBP-GhWAK7A^{CD}, MBP-GhWAK7A$^{K451M\text{-}CD}$, GST-GhCERK1^{CD}, or MBP-GhCERK1^{CD} as kinases were incubated with 10 μg of GST-GhLYK5^{CD} as substrates or other control proteins in 30 μL of kinase buffer (20 mM of Tris-HCl at pH 7.5, 10 mM of $MgCl_2$, 5 mM of EDTA, 100 mM of NaCl, 1 mM of DTT, and 0.1 mM of ATP) with the presence of 5 μCi [^{32}P]-γ-ATP at room temperature for 3 h with gentle shaking. The reactions were stopped by the addition of 4 × SDS loading buffer. The phosphorylation of fusion proteins was analyzed by autoradiography after separation on a 10% SDS-PAGE gel.

In Vivo Kinase Assays

GhLYK5-FLAG was co-transfected with *GhWAK7A-HA*, *GhWAK7A^{K451M}-HA*, or a vector control in 500 μL of cotton protoplasts (2×10^5 cells/mL). Protoplasts were incubated for 12 h and treated with or without 100 μg/mL of chitin for 10 min. Samples were collected and immunoprecipitated with FLAG-agarose beads (Sigma-Aldrich). The beads were collected and washed five times with washing buffer (20 mM of Tris-HCl at pH 7.5, 100 mM of NaCl, 1 mM of EDTA, and 0.2% [v/v] Triton X-100), and once with 50 mM of Tris-HCl at pH 7.5. The immunoprecipitated and input proteins were analyzed by immunoblotting with anti-phosphoSer/Thr antibody (cat. no. PP2551, dilution 1:1,000 [v/v]; ECM Biosciences), α-FLAG (cat. no. A8592, dilution 1:2,000 [v/v]; Sigma-Aldrich), or α-HA (cat. no. 12013819001, dilution 1:2,000 [v/v]; Roche) antibody as indicated.

Statistical Analysis

All data for quantification analyses are presented as mean ± SE or SD. The statistical analyses were performed by two-tailed Student's *t* test or one-way ANOVA test (*$P < 0.05$, **$P < 0.01$). The number of replicates is shown in the figure legends. Statistical results are available in the Supplemental Dataset.

Accession Numbers

Sequence data for the cotton genes described in this article can be found in the databases of *G. hirsutum* (NAU), *G. raimondii* (JGI), and *G. arboreum* (CRI; Paterson et al., 2012; Li et al., 2014; Zhang et al., 2015; https://cottonfgd.org/). The accession numbers are listed in Supplemental Tables 6 and 11 and as follows: *GhRLP2* (Gh_A12G0722), *GhMPK3* (Gh_D03G1283), *GhWRKY30* (Gh_D12G2738), *GhMPK6* (Gh_D02G0105), *GhActin9* (Gh_D04G0254), and *GhUBQ1* (Gh_A10G0147).

Supplemental Data

Supplemental Figure 1. The phylogeny of cotton WAK with AtWAKs and AtWAKLs.

Supplemental Figure 2. Phylogenetic analysis of WAK proteins from cotton (*G. hirsutum*, *G. raimondii*, *G. arboreum*), and Arabidopsis.

Supplemental Figure 3. Phylogenetic analysis of WAK proteins from diploid cotton (*G. raimondii* and *G. arboreum*), and Arabidopsis.

Supplemental Figure 4. The phylogeny of WAK protein kinase domain sequences.

Supplemental Figure 5. Phylogenetic analysis of A-subgenome GhWAKs with GaWAKs, D-subgenome GhWAKs with GrWAKs, and GaWAKs with GrWAKs.

Supplemental Figure 6. The evolutionary relationship of cotton *WAK* genes in *G. hirsutum*, *G. raimondii*, and *G. arboreum*.

Supplemental Figure 7. Conserved residues in EGF_like, EGF_Ca^{2+}, or WAK_GUB domains of GhWAK proteins.

Supplemental Figure 8. GhWAK7A is not involved in drought or salt stress in cotton.

Supplemental Figure 9. Chitin-induced MAPK activation in VIGS-*GhMPK6* and *GhMPK3* cotton.

Supplemental Figure 10. Preparation and characterization of OGs and OG-triggered immune responses in cotton.

Supplemental Figure 11. Chitin-induced MAPK activation and ROS production in Arabidopsis *lyk* mutants.

Supplemental Figure 12. Phylogenetic analysis of LYK proteins from cotton (*G. hirsutum*, *G. raimondii*, *G. arboreum*), and Arabidopsis.

Supplemental Figure 13. The conserved amino acid residues of LsyM motif.

Supplemental Figure 14. Genomic locations of *GhLYK* genes on their corresponding chromosomes of *G. hirsutum* genome.

Supplemental Figure 15. Phylogenetic analysis of A-subgenome GhLYKs with GaLYKs, D-subgenome GhLYKs with GrLYKs, and GaLYKs with GrLYKs.

Supplemental Figure 16. The evolutionary relationship of cotton *LYK* genes in *G. hirsutum*, *G. raimondii*, and *G. arboreum*.

Supplemental Figure 17. The VIGS efficiency of VIGS-*GhLYK4/5* cotton plants and the specific association of GhLYK5 and GhWAK7A via co-IP and the in vitro phosphorylation assay with $GhCERK1^{CD}$ and $GhLYK5^{CD}$.

Supplemental Table 1. Conserved motif prediction of WAK proteins from *G. hirsutum* (NAU assembly).

Supplemental Table 2. Conserved motif prediction of WAK proteins from *G. arboreum* (CRI assembly).

Supplemental Table 3. Conserved motif prediction of WAK proteins from *G. raimondii* (JGI assembly).

Supplemental Table 4. Pair-wise protein identity among GhWAKs and AtWAKs.

Supplemental Table 5. Clade partitions of cotton WAKs.

Supplemental Table 6. Gene IDs and the corresponding gene names of *GhWAK* family.

Supplemental Table 7. Conserved motif prediction of LYK proteins from *G. hirsutum* (NAU assembly).

Supplemental Table 8. Conserved motif prediction of LYK proteins from *G. arboreum* (CRI assembly).

Supplemental Table 9. Conserved motif prediction of LYK proteins from *G. raimondii* (JGI assembly).

Supplemental Table 10. Clade partitions of Arabidopsis and cotton LYKs.

Supplemental Table 11. Gene IDs and the corresponding gene names of the *GhLYK* family.

Supplemental Table 12. Pair-wise protein identity among GhLYKs and AtLYKs.

Supplemental Table 13. The DI of *Vd*-inoculated *GhLYK*-silenced plants from seven repeats.

Supplemental Table 14. The DI of *Fov*-inoculated *GhLYK*-silenced plants from six repeats.

Supplemental Table 15. Primers used in this study.

Supplemental Dataset. Statistical results.

Supplemental File 1. Sequence alignments for Figure 1B.

Supplemental File 2. Machine-readable tree file for Figure 1B.

Supplemental File 3. Sequence alignments for Figure 4C.

Supplemental File 4. Machine-readable tree file for Figure 4C.

ACKNOWLEDGMENTS

We thank Gary Stacey (University of Missouri at Columbia) for the Arabidopsis *cerk1*, *lyk5-2*, and *lyk4*/*lyk5-2* mutant seeds; Terry Wheeler (Texas A&M University) for the *Vd* 'King' isolate strain; Mike Davis (University of California at Davis) for the *Fov* 'CA10' strain; Lijun Ma (University of Massachusetts at Amherst) for the *Fov* '5176' strain; and Liang Kong (Texas A&M University) for the assistance on confocal microscopy and FLIM-FRET assays. This work was supported by the National Institute of Food and Agriculture at the United States Department of Agriculture (grants 2019–67028–29949, 2018–67013–28513, and 2020–67013–31615 to L.S. and P.H.), Texas A&M AgriLife Research (to L.S. and P.H.), Cotton Inc. (grant 18–311 to L.S.), the China Scholar Council (to P.W., L. Zhou, Z.X.Z., S.Y.W., and L.H.W.), and a fellowship from the Pakistan government (to R.M.).

AUTHOR CONTRIBUTIONS

P.W., P.H., and L.S. conceived the study and designed the experiments; P.W., L. Zhou., L. Zhang, Z.X.Z., K.B., W.Y.S., L.H.W., P.J., R.M., A.D., and D.P. performed the experiments; P.W., P.J., L. Zhang, I.A., Y.X.H., S.F., P.H., and L.S. analyzed data; P.W., P.J., and L.S. wrote the article; all authors approved the article.

Received February 25, 2020; revised August 13, 2020; accepted September 30, 2020; published October 9, 2020.

REFERENCES

Appella, E., Weber, I. T., and Blasi, F. (1988). Structure and function of epidermal growth factor-like regions in proteins. FEBS Letters **231:** 1–4.

Ashraf, J., Zuo, D., Wang, Q., Malik, W., Zhang, Y., Abid, M.A., Cheng, H., Yang, Q., and Song, G. (2018). Recent insights into cotton functional genomics: Progress and future perspectives. Plant Biotechnol. J. **16:** 699–713.

Bajar, B.T., Wang, E.S., Zhang, S., Lin, M.Z., and Chu, J. (2016). A guide to fluorescent protein FRET pairs. Sensors (Basel) **16:** 1488.

Benedetti, M., Mattei, B., Pontiggia, D., Salvi, G., Savatin, D.V., and Ferrari, S. (2017). Methods of isolation and characterization of oligogalacturonide elicitors. In Plant Pattern Recognition Receptors: Methods and Protocols, L. Shan, and and P. He, eds (New York, NY: Springer), pp. 25–38.

Böhm, H., Albert, I., Fan, L., Reinhard, A., and Nürnberger, T. (2014). Immune receptor complexes at the plant cell surface. Curr. Opin. Plant Biol. **20:** 47–54.

Brutus, A., Sicilia, F., Macone, A., Cervone, F., and De Lorenzo, G. (2010). A domain swap approach reveals a role of the plant wall-associated kinase 1 (WAK1) as a receptor of oligogalacturonides. Proc. Natl. Acad. Sci. USA **107:** 9452–9457.

Bücherl, C., Aker, J., de Vries, S., and Borst, J.W. (2010). Probing protein–protein interactions with FRET-FLIM. Methods Mol. Biol. **655:** 389–399.

Cao, Y., Liang, Y., Tanaka, K., Nguyen, C.T., Jedrzejczak, R.P., Joachimiak, A., and Stacey, G. (2014). The kinase LYK5 is a major chitin receptor in Arabidopsis and forms a chitin-induced complex with related kinase CERK1. eLife **3:** e03766.

Cianchetta, A.N., and Davis, R.M. (2015). Fusarium wilt of cotton: Management strategies. Crop Prot. **73:** 40–44.

Couto, D., and Zipfel, C. (2016). Regulation of pattern recognition receptor signalling in plants. Nat. Rev. Immunol. **16:** 537–552.

Cox, K.L., Jr., Babilonia, K., Wheeler, T., He, P., and Shan, L. (2019). Return of old foes—recurrence of bacterial blight and Fusarium wilt of cotton. Curr. Opin. Plant Biol. **50:** 95–103.

Davies, D.R., Bindschedler, L.V., Strickland, T.S., and Bolwell, G.P. (2006). Production of reactive oxygen species in *Arabidopsis*

thaliana cell suspension cultures in response to an elicitor from *Fusarium oxysporum*: Implications for basal resistance. J. Exp. Bot. **57:** 1817–1827.

de Jonge, R., van Esse, H.P., Maruthachalam, K., Bolton, M.D., Santhanam, P., Saber, M.K., Zhang, Z., Usami, T., Lievens, B., Subbarao, K.V., and Thomma, B.P. (2012). Tomato immune receptor Ve1 recognizes effector of multiple fungal pathogens uncovered by genome and RNA sequencing. Proc. Natl. Acad. Sci. USA **109:** 5110–5115.

Decreux, A., and Messiaen, J. (2005). Wall-associated kinase WAK1 interacts with cell wall pectins in a calcium-induced conformation. Plant Cell Physiol. **46:** 268–278.

Decreux, A., Thomas, A., Spies, B., Brasseur, R., Van Cutsem, P., and Messiaen, J. (2006). In vitro characterization of the homogalacturonan-binding domain of the wall-associated kinase WAK1 using site-directed mutagenesis. Phytochemistry **67:** 1068–1079.

Delteil, A., Gobbato, E., Cayrol, B., Estevan, J., Michel-Romiti, C., Dievart, A., Kroj, T., and Morel, J.B. (2016). Several wall-associated kinases participate positively and negatively in basal defense against rice blast fungus. BMC Plant Biol. **16:** 17.

Diener, A.C., and Ausubel, F.M. (2005). RESISTANCE TO FUSARIUM OXYSPORUM 1, a dominant Arabidopsis disease-resistance gene, is not race specific. Genetics **171:** 305–321.

Erwig, J., Ghareeb, H., Kopischke, M., Hacke, R., Matei, A., Petutschnig, E., and Lipka, V. (2017). Chitin-induced and CHITIN ELICITOR RECEPTOR KINASE1 (CERK1) phosphorylation-dependent endocytosis of *Arabidopsis thaliana* LYSIN MOTIF-CONTAINING RECEPTOR-LIKE KINASE5 (LYK5). New Phytol. **215:** 382–396.

Faulkner, C., Petutschnig, E., Benitez-Alfonso, Y., Beck, M., Robatzek, S., Lipka, V., and Maule, A.J. (2013). LYM2-dependent chitin perception limits molecular flux via plasmodesmata. Proc. Natl. Acad. Sci. USA **110:** 9166–9170.

Galletti, R., De Lorenzo, G., and Ferrari, S. (2009). Host-derived signals activate plant innate immunity. Plant Signal. Behav. **4:** 33–34.

Gao, W., Long, L., Zhu, L.F., Xu, L., Gao, W.H., Sun, L.Q., Liu, L.L., and Zhang, X.L. (2013a). Proteomic and virus-induced gene silencing (VIGS) analyses reveal that gossypol, brassinosteroids, and jasmonic acid contribute to the resistance of cotton to *Verticillium dahliae*. Mol. Cell. Proteomics **12:** 3690–3703.

Gao, X., Wheeler, T., Li, Z., Kenerley, C.M., He, P., and Shan, L. (2011). Silencing GhNDR1 and GhMKK2 compromises cotton resistance to Verticillium wilt. Plant J. **66:** 293–305.

Gao, X., Li, F., Li, M., Kianinejad, A.S., Dever, J.K., Wheeler, T.A., Li, Z., He, P., and Shan, L. (2013b). Cotton GhBAK1 mediates Verticillium wilt resistance and cell death. J. Integr. Plant Biol. **55:** 586–596.

Gong, B.-Q., Wang, F.-Z., and Li, J.-F. (2020). Hide-and-seek: Chitin-triggered plant immunity and fungal counterstrategies. Trends Plant Sci. **25:** 805–816.

Gonzalez-Cendales, Y., Catanzariti, A.M., Baker, B., Mcgrath, D.J., and Jones, D.A. (2016). Identification of I-7 expands the repertoire of genes for resistance to Fusarium wilt in tomato to three resistance gene classes. Mol. Plant Pathol. **17:** 448–463.

Gu, Z., et al. (2017). Two lysin-motif receptor kinases, Gh-LYK1 and Gh-LYK2, contribute to resistance against *Verticillium wilt* in upland cotton. Front Plant Sci **8:** 2133.

Halter, T., et al. (2014). The leucine-rich repeat receptor kinase BIR2 is a negative regulator of BAK1 in plant immunity. Curr. Biol. **24:** 134–143.

Hayafune, M., et al. (2014). Chitin-induced activation of immune signaling by the rice receptor CEBiP relies on a unique sandwich-type dimerization. Proc. Natl. Acad. Sci. USA **111:** E404–E413.

He, Z.H., Cheeseman, I., He, D., and Kohorn, B.D. (1999). A cluster of five cell wall-associated receptor kinase genes, Wak1-5, are expressed in specific organs of Arabidopsis. Plant Mol. Biol. **39:** 1189–1196.

Hou, X., Tong, H., Selby, J., Dewitt, J., Peng, X., and He, Z.H. (2005). Involvement of a cell wall-associated kinase, WAKL4, in Arabidopsis mineral responses. Plant Physiol. **139:** 1704–1716.

Houterman, P.M., Cornelissen, B.J., and Rep, M. (2008). Suppression of plant resistance gene-based immunity by a fungal effector. PLoS Pathog. **4:** e1000061.

Hu, K., et al. (2017). Improvement of multiple agronomic traits by a disease resistance gene via cell wall reinforcement. Nat. Plants **3:** 17009.

Hu, Q., Zhu, L., Zhang, X., Guan, Q., Xiao, S., Min, L., and Zhang, X. (2018). GhCPK33 negatively regulates defense against *Verticillium dahliae* by phosphorylating GhOPR3. Plant Physiol. **178:** 876–889.

Hu, Y., et al. (2019). *Gossypium barbadense* and *Gossypium hirsutum* genomes provide insights into the origin and evolution of allotetraploid cotton. Nat. Genet. **51:** 739–748.

Huang, C.-C., Huang, C.-C., and Lindhout, P. (1997). Screening for resistance in wild Lycopersicon species to *Fusarium oxysporum* f.sp. *lycopersici* race 1 and race 2. Euphytica **93:** 145–153.

Hurni, S., Scheuermann, D., Krattinger, S.G., Kessel, B., Wicker, T., Herren, G., Fitze, M.N., Breen, J., Presterl, T., Ouzunova, M., and Keller, B. (2015). The maize disease resistance gene Htn1 against northern corn leaf blight encodes a wall-associated receptor-like kinase. Proc. Natl. Acad. Sci. USA **112:** 8780–8785.

Jamieson, P.A., Shan, L., and He, P. (2018). Plant cell surface molecular cypher: Receptor-like proteins and their roles in immunity and development. Plant Sci. **274:** 242–251.

Kaku, H., Nishizawa, Y., Ishii-Minami, N., Akimoto-Tomiyama, C., Dohmae, N., Takio, K., Minami, E., and Shibuya, N. (2006). Plant cells recognize chitin fragments for defense signaling through a plasma membrane receptor. Proc. Natl. Acad. Sci. USA **103:** 11086–11091.

Kanneganti, V., and Gupta, A.K. (2008). Wall associated kinases from plants—an overview. Physiol. Mol. Biol. Plants **14:** 109–118.

Kawasaki, T., Yamada, K., Yoshimura, S., and Yamaguchi, K. (2017). Chitin receptor-mediated activation of MAP kinases and ROS production in rice and Arabidopsis. Plant Signal. Behav. **12:** e1361076.

Kawchuk, L.M., Hachey, J., Lynch, D.R., Kulcsar, F., van Rooijen, G., Waterer, D.R., Robertson, A., Kokko, E., Byers, R., Howard, R.J., Fischer, R., and Prüfer, D. (2001). Tomato Ve disease resistance genes encode cell surface-like receptors. Proc. Natl. Acad. Sci. USA **98:** 6511–6515.

Kohorn, B.D. (2016). Cell wall-associated kinases and pectin perception. J. Exp. Bot. **67:** 489–494.

Kohorn, B.D., and Kohorn, S.L. (2012). The cell wall-associated kinases, WAKs, as pectin receptors. Front Plant Sci **3:** 88.

Kohorn, B.D., Johansen, S., Shishido, A., Todorova, T., Martinez, R., Defeo, E., and Obregon, P. (2009). Pectin activation of MAP kinase and gene expression is WAK2 dependent. Plant J. **60:** 974–982.

Kumar, S., Stecher, G., Li, M., Knyaz, C., and Tamura, K. (2018). MEGA X: Molecular Evolutionary Genetics Analysis across computing platforms. Mol. Biol. Evol. **35:** 1547–1549.

Li, F., Li, M., Wang, P., Cox, K.L., Jr., Duan, L., Dever, J.K., Shan, L., Li, Z., and He, P. (2017a). Regulation of cotton (*Gossypium hirsutum*) drought responses by mitogen-activated protein (MAP) kinase cascade-mediated phosphorylation of GhWRKY59. New Phytol. **215:** 1462–1475.

Li, F., et al. (2014). Genome sequence of the cultivated cotton *Gossypium arboreum*. Nat. Genet. **46:** 567–572.

Li, F., et al. (2015). Genome sequence of cultivated Upland cotton (*Gossypium hirsutum* TM-1) provides insights into genome evolution. Nat. Biotechnol. **33:** 524–530.

Li, X., Zhang, Y., Ding, C., Xu, W., and Wang, X. (2017b). Temporal patterns of cotton Fusarium and Verticillium wilt in Jiangsu coastal areas of China. Sci. Rep. **7:** 12581.

Liu, J., Liu, B., Chen, S., Gong, B.Q., Chen, L., Zhou, Q., Xiong, F., Wang, M., Feng, D., Li, J.F., Wang, H.B., and Wang, J. (2018). A tyrosine phosphorylation cycle regulates fungal activation of a plant receptor Ser/Thr kinase. Cell Host Microbe **23:** 241–253.e6.

Liu, T., Liu, Z., Song, C., Hu, Y., Han, Z., She, J., Fan, F., Wang, J., Jin, C., Chang, J., Zhou, J.M., and Chai, J. (2012). Chitin-induced dimerization activates a plant immune receptor. Science **336:** 1160–1164.

Miya, A., Albert, P., Shinya, T., Desaki, Y., Ichimura, K., Shirasu, K., Narusaka, Y., Kawakami, N., Kaku, H., and Shibuya, N. (2007). CERK1, a LysM receptor kinase, is essential for chitin elicitor signaling in Arabidopsis. Proc. Natl. Acad. Sci. USA **104:** 19613–19618.

Mu, C., Zhou, L., Shan, L., Li, F., and Li, Z. (2019). Phosphatase GhDsPTP3a interacts with annexin protein GhANN8b to reversely regulate salt tolerance in cotton (*Gossypium* spp.). New Phytol. **223:** 1856–1872.

Paterson, A.H., et al. (2012). Repeated polyploidization of Gossypium genomes and the evolution of spinnable cotton fibres. Nature **492:** 423–427.

Petutschnig, E.K., Jones, A.M.E., Serazetdinova, L., Lipka, U., and Lipka, V. (2010). The lysin motif receptor-like kinase (LysM-RLK) CERK1 is a major chitin-binding protein in *Arabidopsis thaliana* and subject to chitin-induced phosphorylation. J. Biol. Chem. **285:** 28902–28911.

Pontiggia, D., Ciarcianelli, J., Salvi, G., Cervone, F., De Lorenzo, G., and Mattei, B. (2015). Sensitive detection and measurement of oligogalacturonides in Arabidopsis. Front Plant Sci **6:** 258.

Rao, Z., Handford, P., Mayhew, M., Knott, V., Brownlee, G. G., and StuartZ, D. (1995). The structure of a Ca^{2+}-binding epidermal growth factor-like domain: Its role in protein-protein interactions. Cell **82:** 131–141.

Riese, J., Ney, J., and Kohorn, B.D. (2018). 7 WAKs: Cell wall associated kinases. In Annual Plant Reviews book series, Volume 8: The Plant Cell Wall, J.K.C. Rose, ed (New York, NY: John Wiley & Sons), pp. 223–236.

Saintenac, C., et al. (2018). Wheat receptor-kinase-like protein Stb6 controls gene-for-gene resistance to fungal pathogen *Zymoseptoria tritici*. Nat. Genet. **50:** 368–374.

Sanogo, S., and Zhang, J.F. (2016). Resistance sources, resistance screening techniques and disease management for Fusarium wilt in cotton. Euphytica **207:** 255–271.

Shen, Y., and Diener, A.C. (2013). *Arabidopsis thaliana* resistance to *Fusarium oxysporum*2 implicates tyrosine-sulfated peptide signaling in susceptibility and resistance to root infection. PLoS Genet. **9:** e1003525.

Shi, G., et al. (2016). The hijacking of a receptor kinase-driven pathway by a wheat fungal pathogen leads to disease. Sci. Adv. **2:** e1600822.

Shimizu, T., Nakano, T., Takamizawa, D., Desaki, Y., Ishii-Minami, N., Nishizawa, Y., Minami, E., Okada, K., Yamane, H., Kaku, H., and Shibuya, N. (2010). Two LysM receptor molecules, CEBiP and OsCERK1, cooperatively regulate chitin elicitor signaling in rice. Plant J. **64:** 204–214.

Shinya, T., Nakagawa, T., Kaku, H., and Shibuya, N. (2015). Chitin-mediated plant-fungal interactions: Catching, hiding and handshaking. Curr. Opin. Plant Biol. **26:** 64–71.

Shiu, S.H., and Bleecker, A.B. (2003). Expansion of the receptor-like kinase/Pelle gene family and receptor-like proteins in Arabidopsis. Plant Physiol. **132:** 530–543.

Tanaka, K., Nguyen, C.T., Liang, Y., Cao, Y., and Stacey, G. (2013). Role of LysM receptors in chitin-triggered plant innate immunity. Plant Signal. Behav. **8:** e22598.

Thatcher, L.F., Gardiner, D.M., Kazan, K., and Manners, J.M. (2012). A highly conserved effector in *Fusarium oxysporum* is required for full virulence on Arabidopsis. Mol. Plant Microbe Interact. **25:** 180–190.

Verica, J.A., and He, Z.H. (2002). The cell wall-associated kinase (WAK) and WAK-like kinase gene family. Plant Physiol. **129:** 455–459.

Verica, J.A., Chae, L., Tong, H., Ingmire, P., and He, Z.H. (2003). Tissue-specific and developmentally regulated expression of a cluster of tandemly arrayed cell wall-associated kinase-like kinase genes in Arabidopsis. Plant Physiol. **133:** 1732–1746.

Veronese, P., Narasimhan, M.L., Stevenson, R.A., Zhu, J.K., Weller, S.C., Subbarao, K.V., and Bressan, R.A. (2003). Identification of a locus controlling Verticillium disease symptom response in *Arabidopsis thaliana*. Plant J. **35:** 574–587.

Wagner, T.A., and Kohorn, B.D. (2001). Wall-associated kinases are expressed throughout plant development and are required for cell expansion. Plant Cell **13:** 303–318.

Wan, J., Zhang, X.C., and Stacey, G. (2008). Chitin signaling and plant disease resistance. Plant Signal. Behav. **3:** 831–833.

Wan, J., Tanaka, K., Zhang, X.C., Son, G.H., Brechenmacher, L., Nguyen, T.H., and Stacey, G. (2012). LYK4, a lysin motif receptor-like kinase, is important for chitin signaling and plant innate immunity in Arabidopsis. Plant Physiol. **160:** 396–406.

Wang, H., Niu, H., Liang, M., Zhai, Y., Huang, W., Ding, Q., Du, Y., and Lu, M. (2019). A wall-associated kinase gene *CaWAKL20* from pepper negatively modulates plant thermotolerance by reducing the expression of ABA-responsive genes. Front Plant Sci **10:** 591.

Wang, K., Wendel, J.F., and Hua, J. (2018). Designations for individual genomes and chromosomes in *Gossypium*. Journal of Cotton Research **1:** 3.

Wang, K., et al. (2012). The draft genome of a diploid cotton *Gossypium raimondii*. Nat. Genet. **44:** 1098–1103.

Wheeler, T.A., Bordovsky, J.P., Keeling, J.W., and Mullinix, B.G., Jr. (2012). Effects of crop rotation, cultivar, and irrigation and nitrogen rate on Verticillium wilt in cotton. Plant Dis. **96:** 985–989.

Xia, Y., Yin, S.J., Zhang, K.L., Shi, X.T., Lian, C.L., Zhang, H.S., Hu, Z.B., and Shen, Z.G. (2018). OsWAK11, a rice wall-associated kinase, regulates Cu detoxification by alteration the immobilization of Cu in cell walls. Environ. Exp. Bot. **150:** 99–105.

Xu, F., Yang, L., Zhang, J., Guo, X.P., Zhang, X.L., and Li, G.Q. (2012). Prevalence of the defoliating pathotype of *Verticillium dahliae* on cotton in central China and virulence on selected cotton cultivars. J. Phytopathol. **160:** 369–376.

Xue, D.X., Li, C.L., Xie, Z.P., and Staehelin, C. (2019). LYK4 is a component of a tripartite chitin receptor complex in *Arabidopsis thaliana*. J. Exp. Bot. **70:** 5507–5516.

Yang, P., Praz, C., Li, B., Singla, J., Robert, C.A.M., Kessel, B., Scheuermann, D., Lüthi, L., Ouzunova, M., Erb, M., Krattinger, S.G., and Keller, B. (2019). Fungal resistance mediated by maize wall-associated kinase ZmWAK-RLK1 correlates with reduced benzoxazinoid content. New Phytol. **221:** 976–987.

Yu, X., Feng, B., He, P., and Shan, L. (2017). From chaos to harmony: Responses and signaling upon microbial pattern recognition. Annu. Rev. Phytopathol. **55:** 109–137.

Yuan, D., et al. (2015). The genome sequence of Sea-Island cotton (*Gossypium barbadense*) provides insights into the allopolyploidization and development of superior spinnable fibres. Sci. Rep. **5:** 17662.

Zhang, B., Yang, Y., Chen, T., Yu, W., Liu, T., Li, H., Fan, X., Ren, Y., Shen, D., Liu, L., Dou, D., and Chang, Y. (2012). Island cotton Gbve1 gene encoding a receptor-like protein confers resistance to both defoliating and non-defoliating isolates of *Verticillium dahliae*. PLoS One **7:** e51091.

Zhang, H.B., Li, Y., Wang, B., and Chee, P.W. (2008). Recent advances in cotton genomics. Int. J. Plant Genomics **2008:** 742304.

Zhang, L., et al. (2018). Long noncoding RNAs involve in resistance to *Verticillium dahliae*, a fungal disease in cotton. Plant Biotechnol. J. **16:** 1172–1185.

Zhang, N., Pombo, M.A., Rosli, H.G., and Martin, G.B. (2020). Tomato wall-associated kinase SlWak1 depends on Fls2/Fls3 to promote apoplastic immune responses to *Pseudomonas syringae*. Plant Physiol. pp.00144.02020.

Zhang, S., Chen, C., Li, L., Meng, L., Singh, J., Jiang, N., Deng, X.W., He, Z.H., and Lemaux, P.G. (2005). Evolutionary expansion, gene structure, and expression of the rice wall-associated kinase gene family. Plant Physiol. **139:** 1107–1124.

Zhang, T., et al. (2015). Sequencing of allotetraploid cotton (*Gossypium hirsutum* L. acc. TM-1) provides a resource for fiber improvement. Nat. Biotechnol. **33:** 531–537.

Zuo, W., et al. (2015). A maize wall-associated kinase confers quantitative resistance to head smut. Nat. Genet. **47:** 151–157.